

Visual correspondence-based explanations improve AI robustness and human-AI team accuracy

Giang Nguyen *
Auburn University
nguyengiangbkhn@gmail.com

Mohammad Reza Taesiri *
University of Alberta
mtaesiri@gmail.com

Anh Nguyen
Auburn University
anh.ng8@gmail.com

Abstract

Explaining artificial intelligence (AI) predictions is increasingly important and even imperative in many high-stakes applications where humans are the ultimate decision makers. In this work, we propose two novel architectures of self-interpretable image classifiers that first explain, and then predict (as opposed to post-hoc explanations) by harnessing the visual correspondences between a query image and exemplars. Our models consistently improve (by 1 to 4 points) on out-of-distribution (OOD) datasets while performing marginally worse (by 1 to 2 points) on in-distribution tests than ResNet-50 and a k -nearest neighbor classifier (kNN). Via a large-scale, human study on ImageNet and CUB, our correspondence-based explanations are found to be more useful to users than kNN explanations. Our explanations help users more accurately reject AI’s wrong decisions than all other tested methods. Interestingly, for the first time, we show that it is possible to achieve complementary human-AI team accuracy (i.e., that is higher than either AI-alone or human-alone), in ImageNet and CUB image classification tasks.

Keywords: Interpretable-by-design, trust calibration, AI-assisted decision making.

1 Introduction

Comparing the input image with training-set exemplars is the backbone for many applications, such as face identification [29], bird identification [17, 75], and image search [75]. This non-parametric approach may improve classification accuracy on out-of-distribution (OOD) data [29, 72, 75, 55] and enables a class of prototype-based explanations [17, 50, 51, 64, 40] that provide insights into the decision making of Artificial Intelligence (AI) systems. Interestingly, prototype-based explanations are more effective in improving human classification accuracy [53, 24, 41] than attribution maps—a common eXplainable AI (XAI) technique in computer vision. Yet, it remains an open question how to make prototype-based XAI classifiers (1) accurate on in-distribution and OOD data and (2) improve human decisions. For example, in face identification, AIs can be confused by partially occluded, never-seen faces and are unable to explain their decisions to users, causing numerous people falsely arrested [5, 7, 3, 6] or wrongly denied of unemployment benefits [1] by the law enforcement.

*Equal contribution. Listing order is random. GN led the development of EMD-Corr and human studies on Gorilla. MRT led the development of CHM-Corr, pilot studies on HuggingFace, and the analysis of human-study data from Gorilla. AN advised the project. All authors contributed to data analysis and paper writing.

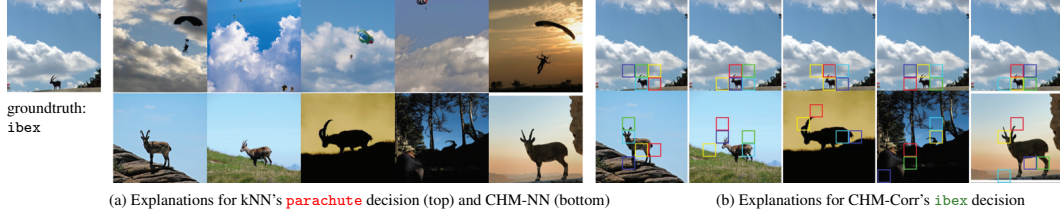


Figure 1: The *ibex* image is misclassified into *parachute* due to its similarity (clouds in blue sky) to *parachute* scenes (a). In contrast, CHM-Corr correctly labels the input as it matches *ibex* images mostly using the animal’s features, discarding the background information (b).

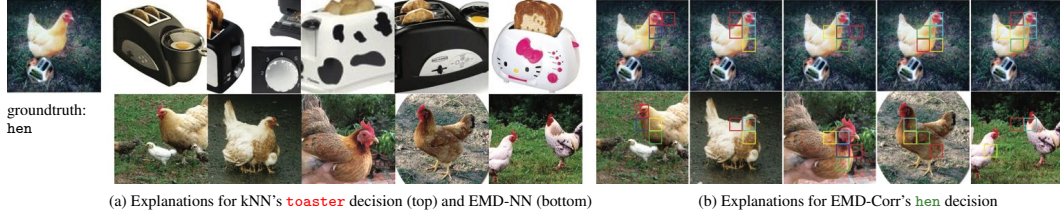


Figure 2: Operating at the image-level visual similarity, kNN incorrectly labels the input *toaster* due to the adversarial toaster patch (a). EMD-Corr instead ignores the adversarial patch and only uses the head and neck patches of the *hen* to make decisions (b).

To address the above questions, we propose two different, *interpretable* [59] classifiers that perform three common steps: (1) rank the training-set images based on their distances to the input using *image-level* features; (2) re-rank the top-50 shortlisted candidates by their *patch-wise* correspondences w.r.t. the input [49, 29]; and then (3) take the dominant class among the top-20 candidates as the predicted label for the input. That is, our classifiers base their decisions on a set of support image-patch pairs, which are also presented as explanations to users (Figs. 1b and 2b). Our main findings include:²

- On ImageNet, a simple k -nearest-neighbor classifier (kNN) based on ResNet-50 features slightly but consistently outperforms ResNet-50 on many OOD datasets (Sec. 3.1). This is further improved after a re-ranking step based on patch-wise similarity (Sec. 3.2).
- Via a large-scale human study, we find visual correspondence-based explanations to improve AI-assisted, human-alone accuracy and human-AI team accuracy on ImageNet and CUB over the baseline kNN explanations (Sec. 3.4).
- Having interpretable AIs label images that they are confident and humans label the rest yields better accuracy than letting AIs or humans alone label all images (Sec. 3.5).

To the best of our knowledge, our work is the first to demonstrate the utility of correspondence-based explanations to users on ImageNet [61] and CUB [69] classification tasks.

2 Methods

2.1 Datasets

We test our ImageNet classifiers on the original 50K-image ILSVRC 2012 ImageNet validation set (i.e., in-distribution data) and four common OOD benchmarks below.

ImageNet-R [35] contains 30K images in 200 ImageNet categories, mostly artworks – ranging from cartoons to video game renditions.

ImageNet-Sketch [70] consists of 50,889 black-and-white sketches of all 1,000 ImageNet classes.

²We release code, model weights, data, and an interactive demo in <https://github.com/anguyen8/visual-correspondence-XAI>.

DAMageNet [18] consists of 50K ImageNet validation-set images but that contain universal, adversarial perturbations for fooling classifiers.

Adversarial Patch [15] are 50K ImageNet validation-set images that are modified to contain an adversarial patch that aims to cause ResNet-50 [31] into labeling every image *toaster* (see Fig. 2). Using the implementation by [2], we generate this dataset, which cause ResNet-50 accuracy to drop from 76.13% to 55.04% (Table 1). See Appendix A.4 for how to download and generate this dataset.

CUB-200-2011 [69] (hereafter, CUB) is a fine-grained, bird-image classification task chosen to complement ImageNet. CUB contains 11,788 images (5,994/5,794 for train/test) of 200 bird species.

2.2 Classifiers

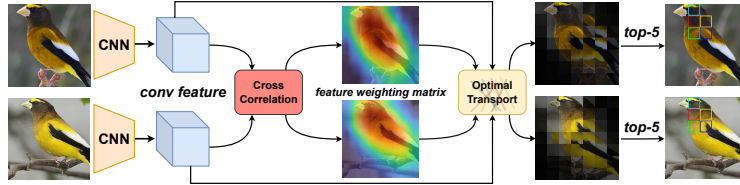
We harness the same ResNet-50 layer4 backbone [8] as the main feature extractor for all four main classifiers, including our two interpretable models. Therefore, to test the effectiveness of our models, we compare them with (1) a vanilla ResNet-50 classifier; and (2) a kNN classifier that uses the same pretrained layer4 features. We report the top-1 accuracy of all classifiers in Table 1.

ResNet-50 For experiments on ImageNet and its four OOD benchmarks, we use the ImageNet-trained ResNet-50 from TorchVision [8] (top-1 accuracy: 76.13%).

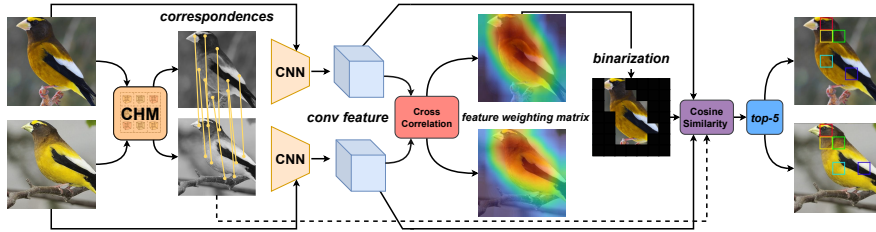
For CUB, we take the ResNet-50 pretrained on iNaturalist [68] from [51] (hereafter, iNaturalist ResNet) and retrain only the last 200-output classification layer (right after avgpool) to create a competitive, baseline ResNet-50 classifier for CUB (top-1 accuracy: 85.83%). See Appendix A.1 for finetuning details.

kNN We implement a vanilla kNN classifier that operates at the avgpool of the last convolutional layer of ResNet-50. That is, given a query image Q , we sort all training-set images $\{G_i\}$ based on their distance $D(Q, G_i)$, which is the cosine distance between the two corresponding image features $f(Q)$ and $f(G_i) \in \mathbb{R}^{512}$ where $f(\cdot)$ outputs the avgpool feature of layer4 (see [code](#)) of ResNet-50.

The predicted label of Q is the dominant class among the top- k images. We choose $k = 20$ as it performs the best among the tested values of $k \in \{10, 20, 50, 100\}$.



(a) EMD-Corr: First compute patch-wise similarity, and then find correspondences via solving EMD [29, 75].



(b) CHM-Corr: First find correspondences via CHM [49], and then compute patch-wise similarity.

Figure 3: EMD-Corr and CHM-Corr both re-rank kNN’s top-50 candidates using the patch-wise similarity between the query and each candidate over the top-5 pairs of patches that are the most important and the most similar (i.e. highest EMD flows in EMD-Corr and highest cosine similarity in CHM-Corr).

EMD-Corr As kNN compares images using only image-level features, it lacks the capability of paying attention to fine details in images. Therefore, we propose EMD-Corr, a visual correspondence-based classifier that (1) re-ranks the top- N (here, $N = 50$) candidates of kNN using their Earth

Mover’s Distance (EMD) with the query in a patch embedding space (see Fig. 3a); and (2), similarly to kNN, takes the dominant class among the re-ranked top-20 as the predicted label.

That is, our PyTorch implementation is the same as that in [75, 29] except for three key differences. First, using layer4 features ($7 \times 7 \times 2048$), we divide an image into 49 patches, whose embeddings are $\in \mathbb{R}^{2048}$. Second, for interpretability, in re-ranking, we only use patch-wise EMD instead of a linear combination of image-level cosine distance and patch-level EMD as in [75, 29], which makes it more opaque how a specific image patch contributes to re-ranking. Third, while the original deep patch-wise EMD [75, 29] between two images (see Eq. 3) is defined as the sum over the *weighted* cosine distances of all 49×49 patch pairs, we only use $L = 5$ pairs as explanations and therefore, only sum over the corresponding 5 flow weights returned by Sinkhorn optimization [21].

We find $N = 50$ to perform the best among $N \in \{50, 100, 200\}$. We choose $L = 5$, which is also the most common in nearest-neighbor visualizations [45, 44]. In preliminary experiments, we find $L = \{9, 16, 25\}$ to yield so dense correspondence visualizations that hurt user interpretation and $L = 3$ to under-inform users. See Appendix A.2 for more description of EMD-Corr.

CHM-Corr EMD-Corr first measures the pair-wise cosine distances for all 49×49 pairs of patches, and then computes the EMD flow weights for these pairs (Fig. 3a). To leverage the recent impressive end-to-end correspondence methods [49, 58, 46], we also propose CHM-Corr (Fig. 3b), a visual correspondence-based classifier that operates in the opposite manner to EMD-Corr. That is, first, we divide the query image Q , into 7×7 non-overlapping patches (i.e. as in EMD-Corr) and find one corresponding patch in G_i for each of the 49 patches of Q using a state-of-the-art correspondence method (here, CHM [49]). Second, for the query Q , we generate a cross-correlation (CC) map (Fig. 3) [29], i.e. a heatmap of cosine similarity scores between the layer4 embeddings of the patches of the query Q and the image-embedding (avgpool after layer4) of each training-set image G_i . Third, we binarize the heatmap (using the optimal threshold $T = 0.55$ found on a held-out training subset) to identify a set of the most important patches in Q and compute the cosine similarity between each such patch and the corresponding patch in G_i (i.e., following the CHM correspondence mappings). Finally, the similarity score $D(Q, G_i)$ in CHM-Corr is the sum over the $L = 5$ patch pairs of the highest cosine similarity across Q and G_i .

After testing NC-Net [58], ANC-Net [46], and CHM [49] in our classifier, we choose CHM as it has the fastest inference speed and the best accuracy. Unlike ResNet-50 [31], which operates at the 224×224 resolution, CHM uses a ResNet-101 backbone that expects a pair of 240×240 images. Therefore, in pre-processing, we resize and center-crop each original ImageNet sample differently according to the input sizes of ResNet-50 and CHM. See Appendix A.3 for more description of CHM-Corr.

CHM-Corr+ classifier based on five groundtruth keypoints of birds In EMD-Corr and CHM-Corr, we use CC to infer the importance weights of patches. To understand the effectiveness of CC in weighting patches, on CUB, we compare our EMD-Corr and CHM-Corr to CHM-Corr+, a CHM-Corr variant where we use a set of five human-defined important patches instead of those inferred by CC. That is, for each CUB image, instead of taking the five CC-derived important patches (Fig. 3b), we use at most five patches that correspond to a set of five pre-defined keypoints (beak, neck, right wing, right feet, tail), each representing a common body part according to bird identification guides [25] for ornithologists. From the five patches in the query image, we then use CHM to find five corresponding patches in a training-set image, and take the of the sum of five cosine similarity as the similarity between two images in re-ranking.

A query image may have fewer than five important patches if some keypoint is occluded. That is, evaluating CHM-Corr+ alone provides an estimate of how hard bird identification on CUB is if the model harnesses five well-known bird features.

2.3 User-study design

The interpretable classifiers (Sec. 2.2) are not only capable of classifying images but also *generating explanations*, which may inform and improve users’ decision-making [53]. Here, we design a large-scale study to understand the effectiveness of explanations in **two human-AI interaction models** in classification (see Fig. 4):

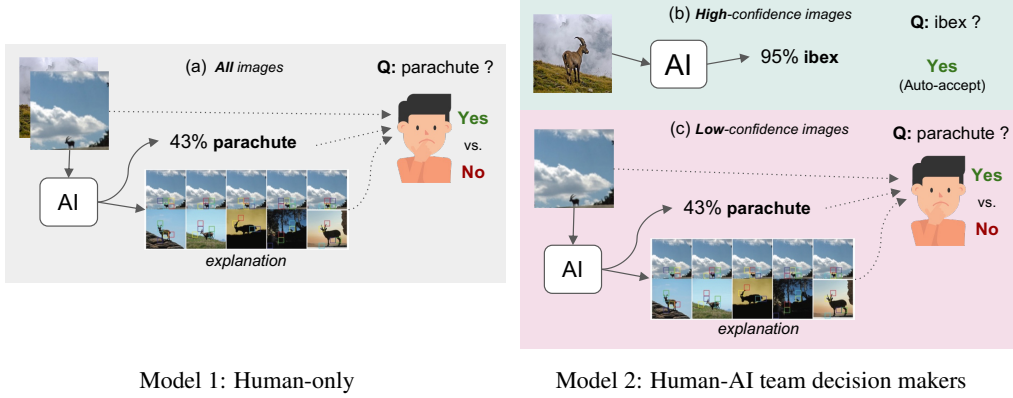


Figure 4: Two human-AI interaction models. In model 1 (a), for all images, users decide (Yes/No) whether the AI’s predicted label is correct given the input image, AI top-1 label and confidence score, and explanations. In model 2, AI decisions are *automatically* accepted if AI is highly confident (b). Otherwise, humans will make decisions (c) in the same fashion as the model 1.

- Model 1: Users make all the decisions after observing the input, AI decisions and explanations (Fig. 4a).
- Model 2: AIs make decisions on only inputs that they are the most confident, leaving the rest for users to label. That is, model 2 (Fig. 4b–c) is a practical scenario where we offload most inputs to AIs while users only handle the harder inputs.

Like [53], we show each user: (1) a query image; (2) AI top-1 label and confidence score; and (3) an explanation (here, available in kNN, EMD-Corr, CHM-Corr, and CHM-Corr+, but not in ResNet-50). We ask users to decide Y/N whether the top-1 label is correct (example screen in Fig. A7).

2.3.1 Explanation methods

We test the explanations of four main classifiers: ResNet-50, kNN, EMD-Corr, and CHM-Corr. Additionally, we test two *ablated* versions (i.e., EMD-NN and CHM-NN) of the explanations of EMD-Corr and CHM-Corr. In total, we test 6 explanation methods (see examples in Appendix C).

ResNet-50 is a representative black-box classifier, which only outputs a top-1 label and a confidence score but *no explanations*.

kNN explanations From the top-20 nearest neighbors (as $k = 20$ in our kNN), we show the first five images that are from the predicted class (example in Fig. 1a). In some cases where the predicted class has only $M < 5$ exemplars in the top-20, we still show only those M images (see Fig. A44). That is, we only show at most five neighbors following prior works [53, 65, 47, 63] that reported utility of such few-image explanations. We find explanations consisting of ≥ 10 images such as those of ProtoPNet [17] are hard to interpret for users [41]. Note that our kNN explanations consist of five support images for each decision of kNN (described in Sec. 2.2) as opposed to the *post-hoc* nearest examples in [53], which do *not* reflect a classifier’s decisions.

EMD-Corr and CHM-Corr explanations As EMD-Corr and CHM-Corr re-rank the top-50 candidates (shortlisted by kNN) and take the dominant class among the resultant top-20 as the predicted label, we show the five nearest neighbors from the predicted class as in kNN explanations. Instead of showing only five post-reranking neighbors, we also annotate, in each image, *all* five patches (example in Fig. 1b and Fig. 2b) that contribute to the patch-wise re-ranking (Sec. 2.2).

EMD-NN and CHM-NN To understand the effects of showing correspondences in the explanations to EMD-Corr and CHM-Corr users, we also test an ablated version where we show exactly the same explanations but without the patch annotations (bottom panels in Fig. 1a and Fig. 2a).

Confidence scores While ResNet-50’s confidence score is the top-1 output softmax probability, the confidence of kNN, EMD-Corr, and CHM-Corr is the count of the predicted-class examples among

the top $k = 20$. In human studies, we display this confidence in percentage (e.g. 10% instead of 2/20; Fig. A44) to be consistent with the confidence score of ResNet-50. Examples of all 6 explanation methods are in Appendix C.

2.3.2 ImageNet and CUB images

For XAI evaluation, we run two human studies, one on ImageNet and one on CUB. For ImageNet, we use ImageNet-ReaL [14] labels in attempt to minimize the confounders of the human evaluation as ImageNet labels are sometimes misleading and inaccurate to users [53].

Nearest-neighbor images To generate the nearest-neighbor explanations for kNN, EMD-Corr, and CHM-Corr, we search for neighbors in the entire training set of ImageNet or CUB (no filtering).

Query images In attempt to ensure the quality of the query images that we ask users to label, from 50K-image ImageNet validation set, we discard images that: (a) do not have an ImageNet ReaL [14] label; (b) are grayscale or low-resolution (i.e., either width or height < 224 px) as in [53]; (c) have duplicates in the ImageNet training set (see Appendix K), resulting in 44,424 images available for sampling for the study. In CUB, we sample from the entire 5,794-image test set and apply no filters.

2.3.3 Training, Validation, and Test phases

From the set of query images (Sec. 2.3.2), we sample images for three phases in a user study: Training, validation, and test. Following [53], we first introduce participants to the task and provide them 5 training examples. Then, each user is given a validation job (10 trials for ImageNet and 5 for CUB), where they must score 100% in order to be invited to our test phase of 30 trials. Otherwise, they will be rejected and unpaid. Among the 10 validation trials for ImageNet, 5 are correctly-labeled and 5 are misclassified by AIs. This ratio is 3/2 for CUB validation (examples in Appendix D.2).

Right before each trial, we describe the top-1 class to participants by showing them 3 training-set images and a 1-sentence WordNet description for each ImageNet class. For CUB classes, we show 6 representative images (instead of 3) for users to better recognize the characteristics of each bird (see Fig. A6).

Sampling For every classifier, we randomly sample 300 correctly and 300 incorrectly predicted images together with their corresponding explanations for the test trials. Over all 6 explanation methods, we have $2 \text{ datasets} \times 600 \text{ images} \times 6 \text{ methods} = 7,200$ test images in total, including both ImageNet and CUB.

2.3.4 Participants

We host human studies on Gorilla [11] and recruit lay participants who are native English speakers worldwide via Prolific [54] at a pay rate of USD 13.5 / hr. We have 360 and 355 users who successfully passed our validation test for ImageNet and CUB datasets, respectively. We remove low-quality, bottom-outlier submissions, i.e., who score ≤ 0.55 (nearly random chance), resulting in 354 and 355 submissions for ImageNet and CUB, respectively. In each dataset, every explanation method is tested on ~ 60 users and each pair of (query, explanation) is seen by almost 3 users (details in Table. 2).

3 Experimental Results

3.1 ImageNet kNN classifiers improve upon ResNet-50 on out-of-distribution datasets

Despite impressive performance on test sets, ImageNet-trained convolutional neural networks (CNNs) may fail to generalize to OOD data or inputs specifically crafted to fool them [52]. It is unknown whether prototype-based classification can leverage the known exemplars (i.e. support images) to generalize better to unseen, rare inputs. To test this question, here, we compare kNN with the baseline ResNet-50 classifier on ImageNet and related ODD datasets (both methods are described in Sec. 2).

On ImageNet and ImageNet-ReaL, kNN performs slightly worse than ResNet-50 by an absolute decrease of **-1.36** and **-0.99** points, respectively (Table 1). However, interestingly, **on all four OOD datasets, kNN consistently outperforms** ResNet-50. Notably, kNN improves upon ResNet-50 by **+1.66** and **+4.26** points on DAmageNet and Adversarial Patch. That is, while ResNet-50 and kNN share the exact same backbone, the kNN’s process of comparing the input image against the

Table 1: Top-1 accuracy (%). **ResNet-50** models’ classification layer is fine-tuned on a specified training set in (b). All other classifiers are non-parametric, nearest-neighbor models based on pretrained ResNet-50 features (a) and retrieve neighbors from the training set (b) during testing. **EMD-Corr** & **CHM-Corr** outperform ResNet-50 models on all OOD datasets (e.g. **+4.39** on Adversarial Patch) and slightly underperform on in-distribution sets (e.g. **-0.72** on ImageNet-Real).

Test set	Features (a)	Training set (b)	ResNet-50	kNN	EMD-Corr	CHM-Corr	CHM-Corr+
ImageNet [61]	ImageNet	ImageNet	76.13	74.77	74.93 (-1.20)	74.40 (-1.73)	n/a
ImageNet-Real [14]	ImageNet	ImageNet	83.04	82.05	82.32 (-0.72)	81.97 (-1.07)	n/a
ImageNet-R [35]	ImageNet	ImageNet	36.17	36.18	37.75 (+1.58)	37.62 (+1.45)	n/a
ImageNet Sketch [70]	ImageNet	ImageNet	24.09	24.72	25.36 (+1.27)	25.61 (+1.52)	n/a
DAmageNet [18]	ImageNet	ImageNet	5.93	7.59	8.16 (+2.23)	8.10 (+2.17)	n/a
Adversarial Patch [15]	ImageNet	ImageNet	55.04	59.30	59.43 (+4.39)	59.86 (+4.82)	n/a
CUB [69]	ImageNet	CUB	n/a	54.72	60.29	53.65	49.63
CUB [69]	iNaturalist [68]	CUB	85.83	85.46	84.98 (-0.85)	83.27 (-2.56)	81.54

training-set examples proves to be beneficial for generalizing to OOD inputs. Intuitively, given the same ImageNet pre-trained feature extractor, it is useful to “look back” at the training-set exemplars again to decide a label for hard, long-tail or OOD samples.

Consistently, using the same CUB-finetuned backbone, kNN is only marginally worse than ResNet-50 on CUB (85.46% vs. 85.83%; Table 1).

3.2 Visual correspondence-based explanations improve kNN robustness further

Recent work found that re-ranking kNN’s shortlisted candidates using the patch-wise similarity between the query and training set examples can further improve classification accuracy on OOD data for some image matching tasks [29, 75, 72] such as face identification [29]. Furthermore, patch-level comparison is also useful in prototype-based bird classifiers [17, 22]. Inspired by these prior successes and the fact that EMD-Corr and CHM-Corr base the patch-wise similarity of two images on only 5 pairs of patches instead of all $49 \times 49 = 2,401$ pairs as in [29, 75, 72], here we test whether our two proposed re-rankers are able to improve the test-set accuracy and robustness over kNN.

Experiment We run EMD-Corr and CHM-Corr on all datasets and compare their results with that of kNN (Table 1). Both methods (described in Sec. 2) re-rank the top $N = 50$ shortlisted candidates returned by kNN and then take the dominant class in the top- k (where $k = 20$) as the predicted label.

ImageNet results Interestingly, despite using only 5 pairs of patches to compute image similarity for re-ranking, both classifiers consistently improve upon kNN further, especially in all OOD datasets. Overall, EMD-Corr and CHM-Corr outperform kNN and ResNet-50 baselines from **+1.27** to **+4.82** points (Table 1). Intuitively, in some hard cases where the main object is small, the two Corr classifiers ignore irrelevant patches (e.g. the sky in ibex images; Fig. 1) and only use the five most relevant patches to make decisions. Similarly, on Adversarial Patch, relying on a few key patches while ignoring adversarial patches enables our classifiers to outperform baselines (Fig. 2). See Appendix H for many qualitative examples comparing Corr and kNN predictions.

CUB results Interestingly, using the same ImageNet-pretrained backbones, EMD-Corr outperforms kNN by an absolute **+5.57** points when tested on CUB (60.29% vs. 54.72%; Table 1). However, this difference vanishes when using CUB-pretrained backbones (Table 1; 84.98% vs. 85.46%).

Our CUB results and ImageNet results are consistent and together reveal a trend: On i.i.d test sets, Corr models perform on par with kNN; however, on OOD images, they consistently outperform kNN, highlighting the benefits of patch-wise comparison.

3.3 CHM-Corr leverages five patches that are more important than five bird keypoints

EMD-Corr and CHM-Corr harness five patches per image for computing a patch-wise similarity score for a pair of images (Sec. 2.2). As these five patches are automatically inferred by cross-correlation (Fig. 3), it is interesting to understand further whether replacing these five patches by five user-defined key patches would improve classification accuracy.

Experiment Since there are no keypoints provided for ImageNet, we test the importance of the five key patches chosen by Corr methods on CUB because CUB provides ornithologist-defined

annotations for each bird image. That is, we create a baseline CHM-Corr+, which is the same as CHM-Corr, except that we use five important patches that correspond to five keypoints in a bird image—beak, belly, tail, right wing, and right foot—as described in Sec. 2.2. We also test CHM-Corr+ sweeping across the number of keypoints $\in \{5, 10, 15\}$.

Results On CUB, CHM-Corr outperforms CHM-Corr+ despite the baseline method leverages **five** known bird keypoints (Table 1; 83.27% vs. 81.51%) while CHM-Corr may use also background patches. Interestingly, when increasing the number of keypoints to 10 and 15, the accuracy of CHM-Corr+ is still lower than that of CHM-Corr (i.e., from 81.51% to 82.34% and 82.27%, respectively). That is, 15 keypoints may correspond to at most 15 different patches per image (if each keypoint lies in a unique, non-overlapping patch among the total of 49 patches per image).

Our results show strong evidence that the five key patches inferred by CC used in EMD- and CHM-Corr are more important than bird keypoints and do not necessarily cover the bird. Qualitative comparisons between CHM-Corr and CHM-Corr+ predictions are in Appendix I.

3.4 On ImageNet-Real, correspondence-based explanations are more useful to users than kNN explanations

Given that EMD-Corr and CHM-Corr classifiers outperform kNN classifiers on OOD datasets (Sec. 3.2), it is an interesting to test how their respective explanations help humans perform classification on ImageNet. Furthermore, in image classification, kNN explanations were found to be more useful to humans than saliency maps [53].

Experiment We perform a human study to assess the ImageNet-Real classification accuracy of *users* of each classifier (described in Sec. 2.2) when they are provided with a classifier’s predictions and explanations. That is, we measure the AI-assisted classification accuracy of users following human-AI interaction model 1 (Fig. 4a). We compare the accuracy between user groups of four classifiers ResNet-50, kNN, EMD-Corr, and CHM-Corr (described in Sec. 2.3.1).

Additionally, to thoroughly assess the impact of showing the correspondence boxes compared to showing only nearest neighbor images (CHM-Corr vs. CHM-NN in Fig. 1), we test two more user groups of EMD-NN and CHM-NN, i.e. the same explanations as of those of the Corr classifiers but with the correspondence boxes hidden.

Results First, the mean accuracy of kNN users is consistently lower than that of the other models’ users (e.g., 75.76% vs. 78.87% of EMD-Corr; Table 2). The EMD-Corr improvement over kNN is statistically significant ($p < 0.01$ via Mann-Whitney U test; Fig. 5a)

Second, interestingly, we find the differences between EMD-, CHM-Corr and their respective baselines are small and not statistically significant (Fig. 5a). That is, on ImageNet-Real, quantitatively, showing the correspondence boxes on top of nearest neighbors is not more useful to users. Third, surprisingly, the users of ResNet-50 (mean accuracy of 81.56%; Table 2) outperform all other methods’ users, suggesting that on ImageNet, a task of many familiar classes to users, *ante-hoc* explanations hurt user accuracy rather than help. Note that in Nguyen et al. [53], post-hoc kNN explanations was found useful to humans compared to not showing any explanations. Yet, here, each classifier’s users are provided with a different set of images and AI decisions, which can also influence the user accuracy. When ResNet-50 is wrong, their users are substantially better in detecting such misclassifications compared to other models’ users (Fig. A11a).

3.5 On CUB fine-grained bird classification, correspondence-based explanations are the most useful to users, helping them to more accurately reject AI misclassifications

To assess whether the findings on ImageNet-Real in Sec. 3.4 generalize to a fine-grained classification task, we repeat the user study on CUB—which is considered much harder to lay users than ImageNet.

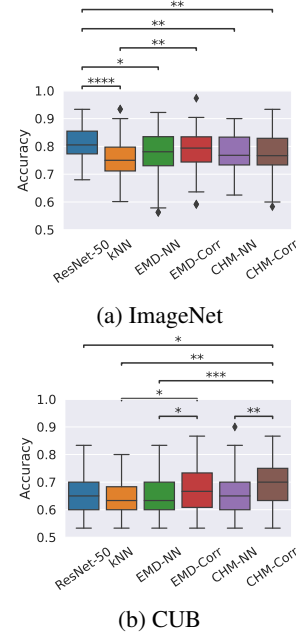


Figure 5: Mann-Whitney U test of the user accuracy scores of 6 methods. * = p -value < 0.05 . ** = p -value < 0.01 . *** = p -value < 0.001 .

Table 2: Human-only accuracy (%)

Method	ImageNet-Real		CUB	
	Users	Accuracy	Users	Accuracy
ResNet-50	60	81.56 \pm 5.54	60	65.50 \pm 7.46
kNN	59	75.76 \pm 8.55	59	64.75 \pm 7.14
EMD-Corr	59	78.87 \pm 6.57	58	67.64 \pm 7.44
CHM-Corr	59	77.23 \pm 7.56	59	69.72 \pm 9.08
EMD-NN	57	77.72 \pm 8.27	59	64.12 \pm 7.07
CHM-NN	60	77.56 \pm 6.91	60	65.72 \pm 8.14

Table 3: AI-only and Human-AI team accuracy (%)

Method	ImageNet-Real		CUB	
	AI-only	Human-AI	AI-only	Human-AI
ResNet-50	86.05	90.41 (+4.36)	87.11	87.74 (+0.63)
kNN	85.95	87.85 (+1.90)	87.40	86.56 (-0.84)
EMD-Corr	85.91	89.48 (+3.57)	86.88	87.03 (+0.15)
CHM-Corr	85.36	88.51 (+3.15)	85.48	87.22 (+1.74)
<i>mean</i>	85.18	89.06 (+3.88)	86.18	87.14 (+0.96)

Results Interestingly, we find EMD-Corr and CHM-Corr users consistently outperform ResNet-50, kNN, EMD-NN, and CHM-NN users (Table 2). The differences between EMD-Corr (or CHM-Corr) and every other baseline is statistically significant ($p < 0.05$ via Mann-Whitney U test; Fig. 5b). That is, on CUB, the visual correspondence boxes helps users make more accurate decisions compared to (a) having no explanations at all (ResNet-50); (b) showing nearest neighbors sorted by image similarity only, not patch correspondences (Fig. 1a; kNN); and (c) having patch-wise correspondence neighbors but not displaying the boxes (Fig. A37; CHM-NN and EMD-NN).

Corr explanations help users reject AI misclassifications while kNN is poorly trust-calibrated

In attempt to understand why the two Corr classifiers help users the most, we find that EMD-Corr and CHM-Corr users reject AI predictions at the highest rates (32.70% and 33.73%; Table A5) while kNN users reject the least (18.47%).

This might have led to the substantially higher top-1 accuracy of CHM-Corr, compared to all other models’ user groups, when *AI predictions are wrong* (Fig. A11b; e.g., 53.45% CHM-Corr accuracy vs. 41.22% of ResNet-50). That is, CHM-Corr users correctly reject 53.45% of the images that the CHM-Corr classifier mislabels. In contrast, kNN users reject the least, only 33.22% of incorrect predictions (Fig. A11b). kNN explanations tend to fool users into accepting the kNN’s wrong decisions (Fig. 6)—the accuracy of kNN users is 33.22%, much lower than the 41.22% of ResNet-50 users who observe no explanations. On ImageNet (Fig. A11), kNN is also poorly “trust-calibrated” [67, 71].

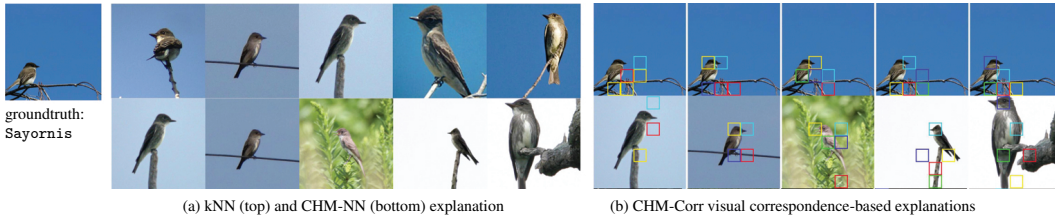


Figure 6: A Sayornis bird image is **misclassified** into Olive Sided Flycatcher by both kNN and CHM-Corr models. Yet, all 3/3 CHM-Corr users **correctly rejected** the AI prediction while 4/4 kNN users **wrongly accepted**. CHM-Corr explanations (b) show users more diverse samples and more evidence against the AI’s decision. More similar examples are in Appendix G.1.

We hypothesize that kNN explanations tend to fool users more as their nearest neighbors, by design, show images that are *image-wise* similar to the query (regardless of whether the kNN prediction is correct or not) while EMD-Corr and CHM-Corr re-rank the images based on *patch-wise* similarity. Furthermore, we find the **images in kNN explanations are also less diverse** than those in Corr explanations both in LPIPS and MS-SSIM (Appendix G.2). Corr explanations tend to include more diverse images (Fig. 6a; top vs. bottom) and provide users with more contrastive evidence in order to reject AI’s incorrect predictions.

Additionally, we also hypothesize that users are less confident in AI’s decisions (and thus reject more) when Corr explanations show some background and uninformative patches used in the matching process (e.g., the 1st and 4th image in Fig. 6b). Yet, such boxes are not available in kNN explanations.

When Corr explanations allow for more disagreement between AI and users, humans also tend to incorrectly reject AI’s correct predictions more often (Fig. A11b; Corr users are the least accurate among 6 methods when the AI is correct). EMD-Corr and CHM-Corr users score ~ 4 points

below ResNet-50 users (84.94% and 85.99% vs. 89.87% of ResNet-50). When most users reject AI’s correct predictions, we observe that some discriminative features (e.g., the belly stripes of the field sparrows; Fig. A33c) are often occluded in the query, leading to human-AI disagreement.

3.6 Human-AI teams outperform both AIs alone and humans alone

In Sec. 3.5, we find that user classification accuracy can be improved when humans are provided with AI predictions and explanations. Here, we leverage the same data collected from the previous ImageNet-ReaL and CUB human studies (Secs. 3.4 and 3.5) to estimate the accuracy of a human-AI team that allow both humans and AIs to make final decisions (Fig. 4; Model 2).

That is, AIs make binary Yes/No predictions on all the $X\%$ of images that they assign a high confidence score $\geq T$ where $T \in [0, 1]$ (Fig. 4b). Given these images and AI predictions, we compute an accuracy score acc_{AI} . For the set of remaining images (i.e. whose AI confidence is $< T$), we take their users’ predictions and also compute an accuracy score $\text{acc}_{\text{human}}$. We define the human-AI team accuracy acc_{team} as:

$$\text{acc}_{\text{team}} = X\% \times \text{acc}_{\text{AI}} + (100 - X)\% \times \text{acc}_{\text{human}}$$

As the interaction model 2 is more practical and scalable, it is interesting to test how the acc_{team} compares with the accuracy when users or AIs alone classify all images (i.e. when $X = 0$ or 100).

Experiment For each classifier (ResNet-50, kNN, EMD-Corr, and CHM-Corr), we use a 2K-image held-out subset of the ImageNet validation³ set to find an optimal threshold T that maximizes the classifier’s binary classification accuracy. Then, we use the remaining $\sim 42\text{K}$ ImageNet validation images for testing. For CUB, we tune T using 1K test images and test on the remaining $\sim 4.7\text{K}$ test-set images.

After obtaining an AI accuracy score for each value of $T \in \{0.05, 0.10, 0.15, \dots, 0.95\}$, we find the best acc_{team} (at an optimal T^*) and repeat the same process to find the best AI-only accuracy. More details of the sweeps are in Appendix F.

Results First, across all four classifiers and two datasets, AI-only accuracy is consistently higher than human-only accuracy (Table 3 vs. Table 2). That is, letting users make all the AI-assisted decisions is both more labor-intensive and less accurate compared to letting AIs classify all the data themselves. This result is consistent with the prior studies that find AIs to outperform humans [28, 74, 57, 26] (see [12] for a summary).

Second, interestingly, human-AI teams consistently outperform the AIs alone (Table 3) and humans alone (Table 2). That is, lay-users may be considered “expert” on ImageNet’s everyday objects and therefore, when teaming up with humans to form human-AI teams, the accuracy substantially increases on average by +3.88 (Table 3). On CUB, which is more challenging to lay-users, this benefit of teaming up with users is smaller (Table 3; +0.96)

Third, among four classifiers, ResNet-50 yields the highest human-AI team accuracy on both ImageNet-ReaL and CUB (Table 3). However, the variance in team accuracy across the classifiers is small. Our results interestingly imply that while there is a significant evidence that Corr explanations are useful to the AI-assisted decision making of humans in the interaction model 1 (Table 2; CUB), such benefits of XAI models average out in the interaction model 2.

4 Related Work

Patch-wise similarity Calculating patch-wise similarity, either intra-image [23] or inter-image [29, 75, 72], has been useful in many tasks as the comparison enables machines to attend to fine-grained details and compute more accurate decisions. Our EMD-Corr harnesses a similar approach to that in [29, 75]; which, however, was not tested on ImageNet classification as in our work. Furthermore, we only compute the total patch-wise similarity over the top-5 patch pairs between the query and each exemplar instead of all pairs as in [29, 75]. Compared to recent patch-wise similarity

³Because the training set is used by non-parametric classifiers during testing, we tune T using 2K-image validation images for ImageNet or 1K test images for CUB.

works that use either cross-attention in ViTs [23] or EMD [75, 72, 29, 42], our work is the first to perform human evaluation of the correspondence-based explanations.

Prototype-based XAI methods Our work is motivated by the recent finding that exemplar-based explanations are more effective than heatmap-based explanations in improving human classification accuracy [53, 38, 41, 24]. However, showing an entire image as an exemplar without any further localization may be confusing as it is unknown which parts of the image the AI is paying attention to [53, 38]. Our EMD-Corr and CHM-Corr present a novel combination of heatmap-based and prototype-based XAI approaches. None of the prior prototype-based XAI methods that operate at the patch level [17, 51, 75, 22] (see Table 3 in [22]) were tested on humans yet. Also, in preliminary tests, we find their explanation formats too dense (i.e., showing over 10 prototypes [17], 9 correspondence pairs per image [22], or an entire prototype tree to humans [50, 51]) to be useful for lay users in practice.

Another major difference is that our Corr classifiers are nonparametric, allowing the training set to be adjusted or swapped with any external knowledgebase for debugging purposes. In contrast, recent prototype-based classifiers [17, 51, 75, 22] are parametric, using a set of learned prototypes and thus may not perform well on OOD datasets as EMD-Corr and CHM-Corr.

Post-hoc prototype-based explanations Some prototype-based methods are post-hoc [40, 53, 20], i.e., generating explanations to explain a decision after-the-fact, which could be highly unfaithful [59, 60]. Instead, our approach is inherently interpretable [60], i.e., retrieving the patches first, and then using them to make classification decisions. While our binary classification task is adopted from [53], our study compares 4 different classifiers while Nguyen et al. [53] instead tested a single classifier with multiple post-hoc explanations.

Human studies Our study has 709 users in total, i.e. ~ 60 users per method per dataset, which is substantially larger than that in most prior works. That is, ~ 30 and 40 users per method participated in [53] and in [47], respectively while Adebayo et al. [9] had 54 persons in total for the entire study of multiple methods.

Human-AI teaming Human-AI collaboration is becoming more essential in the modern AI era [32]. A large body of prior works have investigated such collaboration in other domains (e.g., NLP [12, 73], healthcare [16] and others [33, 16, 74, 19]); however, only few works investigated human-AI collaboration in the image classification setting [53, 41, 24].

Some prior works predict when to defer the decision-making to humans [56, 37, 39]. However, by simply offloading input instances onto humans based on the predicted confidence score associated with the top-1 label, we achieve complementary human-AI team performance in both ImageNet and CUB. Previous works [12, 62] found that algorithmic explanations benefit human decision-making in general, but did not find XAI methods to yield team complementary performance [32], which we report in this work.

5 Discussion and Conclusion

Limitations Due to the limited amount of time and expensive cost of computation related to EMD-Corr or CHM-Corr, we did not experiment on a wider range of OOD datasets (e.g., adversarial poses [10]). We tested our methods on ImageNet-A [36], ObjectNet [13], and ImageNet-C [34] as well, but in a small scale of 5K-image sets (see Table. A2). As using online crowdworkers for the XAI human evaluation, we share the same limitations with [53]. That is, despite our best efforts to minimize biases, the human data quality can be improved in highly-controlled laboratory conditions like in [27]. Algorithm-wise, EMD-Corr and CHM-Corr are re-ranking methods and therefore run substantially slower than ResNet-50.

In conclusion, our work is the first attempt to: (1) study the effectiveness of patch-wise comparison in improving the robustness of deep image classifiers on ImageNet OOD benchmarks; (2) show the utility of visual correspondence-based explanations in assisting users make more accurate decisions downstream image classification tasks; (3) achieve human-AI complementary team performance in the image domain.

References

- [1] The pandemic is testing the limits of face recognition | mit technology review. <https://www.technologyreview.com/2021/09/28/1036279/pandemic-unemployment-government-face-recognition/>. (Accessed on 11/09/2021). 1
- [2] jhayes14/adversarial-patch: Pytorch implementation of adversarial patch. <https://github.com/jhayes14/adversarial-patch>. (Accessed on 05/18/2022). 3, 19
- [3] Wrongfully arrested man sues detroit police following false facial-recognition match - the washington post. <https://www.washingtonpost.com/technology/2021/04/13/facial-recognition-false-arrest-lawsuit/>. (Accessed on 11/09/2021). 1
- [4] M-nauta/prototree: Prototrees: Neural prototype trees for interpretable fine-grained image recognition, published at cvpr2021. <https://github.com/M-Nauta/ProtoTree>. (Accessed on 06/14/2022). 17
- [5] The new lawsuit that shows facial recognition is officially a civil rights issue | mit technology review. <https://www.technologyreview.com/2021/04/14/1022676/robert-williams-facial-recognition-lawsuit-aclu-detroit-police/>. (Accessed on 04/15/2021). 1
- [6] Michigan man wrongfully accused with facial recognition urges congress to act. <https://www.detroitnews.com/story/news/politics/2021/07/13/house-panel-hear-michigan-man-wrongfully-accused-facial-recognition/7948908002/>. (Accessed on 11/09/2021). 1
- [7] Flawed facial recognition leads to arrest and jail for new jersey man - the new york times. <https://www.nytimes.com/2020/12/29/technology/facial-recognition-misidentify-jail.html>. (Accessed on 11/09/2021). 1
- [8] vision at master · pytorch/vision. <https://github.com/pytorch/vision/blob/master/torchvision/models>. (Accessed on 05/08/2022). 3, 17, 18
- [9] Adebayo, J., Muelly, M., Liccardi, I., and Kim, B. Debugging tests for model explanations. *Advances in Neural Information Processing Systems*, 33:700–712, 2020. 11
- [10] Alcorn, M. A., Li, Q., Gong, Z., Wang, C., Mai, L., Ku, W.-S., and Nguyen, A. Strike (with) a pose: Neural networks are easily fooled by strange poses of familiar objects. In *Proceedings of the IEEE Conference on Computer Vision and Pattern Recognition*, pp. 4845–4854, 2019. 11
- [11] Anwyl-Irvine, A. L., Massonnié, J., Flitton, A., Kirkham, N., and Evershed, J. K. Gorilla in our midst: An online behavioral experiment builder. *Behavior research methods*, 52(1):388–407, 2020. 6
- [12] Bansal, G., Wu, T., Zhou, J., Fok, R., Nushi, B., Kamar, E., Ribeiro, M. T., and Weld, D. Does the whole exceed its parts? the effect of ai explanations on complementary team performance. In *Proceedings of the 2021 CHI Conference on Human Factors in Computing Systems*, pp. 1–16, 2021. 10, 11
- [13] Barbu, A., Mayo, D., Alverio, J., Luo, W., Wang, C., Gutfreund, D., Tenenbaum, J., and Katz, B. Objectnet: A large-scale bias-controlled dataset for pushing the limits of object recognition models. *Advances in neural information processing systems*, 32, 2019. 11, 20
- [14] Beyer, L., Hénaff, O. J., Kolesnikov, A., Zhai, X., and Oord, A. v. d. Are we done with imagenet? *arXiv preprint arXiv:2006.07159*, 2020. 6, 7
- [15] Brown, T. B., Mané, D., Roy, A., Abadi, M., and Gilmer, J. Adversarial patch. *arXiv preprint arXiv:1712.09665*, 2017. 3, 7, 19
- [16] Caruana, R., Lou, Y., Gehrke, J., Koch, P., Sturm, M., and Elhadad, N. Intelligible models for healthcare: Predicting pneumonia risk and hospital 30-day readmission. In *Proceedings of the 21th ACM SIGKDD international conference on knowledge discovery and data mining*, pp. 1721–1730, 2015. 11
- [17] Chen, C., Li, O., Tao, D., Barnett, A., Rudin, C., and Su, J. K. This looks like that: deep learning for interpretable image recognition. *Advances in neural information processing systems*, 32, 2019. 1, 5, 7, 11
- [18] Chen, S., He, Z., Sun, C., Yang, J., and Huang, X. Universal adversarial attack on attention and the resulting dataset damagenet. *IEEE Transactions on Pattern Analysis and Machine Intelligence*, 2020. 3, 7, 20
- [19] Chu, E., Roy, D., and Andreas, J. Are visual explanations useful? a case study in model-in-the-loop prediction. *arXiv preprint arXiv:2007.12248*, 2020. 11

- [20] Crabbé, J., Qian, Z., Imrie, F., and van der Schaar, M. Explaining latent representations with a corpus of examples. *Advances in Neural Information Processing Systems*, 34, 2021. 11
- [21] Cuturi, M. Sinkhorn distances: Lightspeed computation of optimal transport. *Advances in neural information processing systems*, 26, 2013. 4, 18
- [22] Donnelly, J., Barnett, A. J., and Chen, C. Deformable protopnet: An interpretable image classifier using deformable prototypes. *arXiv preprint arXiv:2111.15000*, 2021. 7, 11
- [23] Dosovitskiy, A., Beyer, L., Kolesnikov, A., Weissenborn, D., Zhai, X., Unterthiner, T., Dehghani, M., Minderer, M., Heigold, G., Gelly, S., Uszkoreit, J., and Houlsby, N. An image is worth 16x16 words: Transformers for image recognition at scale. In *International Conference on Learning Representations*, 2021. URL <https://openreview.net/forum?id=YicbFdNTTy>. 10, 11
- [24] Fel, T., Colin, J., Cadène, R., and Serre, T. What i cannot predict, i do not understand: A human-centered evaluation framework for explainability methods. *arXiv preprint arXiv:2112.04417*, 2021. 1, 11
- [25] Feng, H., Wang, S., and Ge, S. S. Fine-grained visual recognition with salient feature detection. *arXiv preprint arXiv:1808.03935*, 2018. 4
- [26] Feng, S. and Boyd-Graber, J. What can ai do for me? evaluating machine learning interpretations in cooperative play. In *Proceedings of the 24th International Conference on Intelligent User Interfaces*, pp. 229–239, 2019. 10
- [27] Geirhos, R., Narayanappa, K., Mitkus, B., Thieringer, T., Bethge, M., Wichmann, F. A., and Brendel, W. Partial success in closing the gap between human and machine vision. *Advances in Neural Information Processing Systems*, 34, 2021. 11
- [28] Ghaeini, R., Fern, X. Z., and Tadepalli, P. Interpreting recurrent and attention-based neural models: a case study on natural language inference. *arXiv preprint arXiv:1808.03894*, 2018. 10
- [29] Hai Phan, A. N. Deepface-emd: Re-ranking using patch-wise earth mover’s distance improves out-of-distribution face identification. In *Proceedings of the IEEE/CVF Conference on Computer Vision and Pattern Recognition*, 2022. 1, 2, 3, 4, 7, 10, 11, 17, 18
- [30] Ham, B., Cho, M., Schmid, C., and Ponce, J. Proposal flow: Semantic correspondences from object proposals. *IEEE transactions on pattern analysis and machine intelligence*, 40(7):1711–1725, 2017. 18
- [31] He, K., Zhang, X., Ren, S., and Sun, J. Deep residual learning for image recognition. In *Proceedings of the IEEE conference on computer vision and pattern recognition*, pp. 770–778, 2016. 3, 4, 19
- [32] Hemmer, P., Schemmer, M., Vössing, M., and Kühl, N. Human-ai complementarity in hybrid intelligence systems: A structured literature review. *PACIS 2021 Proceedings*, 2021. 11
- [33] Hemmer, P., Schemmer, M., Kühl, N., Vössing, M., and Satzger, G. On the effect of information asymmetry in human-ai teams. *arXiv preprint arXiv:2205.01467*, 2022. 11
- [34] Hendrycks, D. and Dietterich, T. Benchmarking neural network robustness to common corruptions and perturbations. *arXiv preprint arXiv:1903.12261*, 2019. 11, 20
- [35] Hendrycks, D., Basart, S., Mu, N., Kadavath, S., Wang, F., Dorundo, E., Desai, R., Zhu, T., Parajuli, S., Guo, M., et al. The many faces of robustness: A critical analysis of out-of-distribution generalization. In *Proceedings of the IEEE/CVF International Conference on Computer Vision*, pp. 8340–8349, 2021. 2, 7, 20
- [36] Hendrycks, D., Zhao, K., Basart, S., Steinhardt, J., and Song, D. Natural adversarial examples. In *Proceedings of the IEEE/CVF Conference on Computer Vision and Pattern Recognition*, pp. 15262–15271, 2021. 11, 20
- [37] Horvitz, E. and Paek, T. Complementary computing: policies for transferring callers from dialog systems to human receptionists. *User Modeling and User-Adapted Interaction*, 17(1):159–182, 2007. 11
- [38] Jeyakumar, J. V., Noor, J., Cheng, Y.-H., Garcia, L., and Srivastava, M. How can i explain this to you? an empirical study of deep neural network explanation methods. *Advances in Neural Information Processing Systems*, 33:4211–4222, 2020. 11
- [39] Kamar, E., Hacker, S., and Horvitz, E. Combining human and machine intelligence in large-scale crowdsourcing. In *AAMAS*, volume 12, pp. 467–474, 2012. 11

- [40] Kenny, E. M. and Keane, M. T. Twin-systems to explain artificial neural networks using case-based reasoning: Comparative tests of feature-weighting methods in ann-cbr twins for xai. In *Twenty-Eighth International Joint Conferences on Artificial Intelligence (IJCAI), Macao, 10-16 August 2019*, pp. 2708–2715, 2019. 1, 11
- [41] Kim, S. S., Meister, N., Ramaswamy, V. V., Fong, R., and Russakovsky, O. Hive: Evaluating the human interpretability of visual explanations. *arXiv preprint arXiv:2112.03184*, 2021. 1, 5, 11
- [42] Kim, W., Son, B., and Kim, I. Vilt: Vision-and-language transformer without convolution or region supervision. In *International Conference on Machine Learning*, pp. 5583–5594. PMLR, 2021. 11
- [43] Kingma, D. P. and Ba, J. Adam: A method for stochastic optimization. *arXiv preprint arXiv:1412.6980*, 2014. 17
- [44] Krizhevsky, A., Sutskever, I., and Hinton, G. E. Imagenet classification with deep convolutional neural networks. *Advances in neural information processing systems*, 25, 2012. 4
- [45] Li, H., Wang, Y., Wu, A., Wei, H., and Qu, H. Structure-aware visualization retrieval. In *CHI Conference on Human Factors in Computing Systems*, pp. 1–14, 2022. 4
- [46] Li, S., Han, K., Costain, T. W., Howard-Jenkins, H., and Prisacariu, V. Correspondence networks with adaptive neighbourhood consensus. In *Proceedings of the IEEE/CVF Conference on Computer Vision and Pattern Recognition*, pp. 10196–10205, 2020. 4
- [47] Mac Aodha, O., Su, S., Chen, Y., Perona, P., and Yue, Y. Teaching categories to human learners with visual explanations. In *Proceedings of the IEEE Conference on Computer Vision and Pattern Recognition*, pp. 3820–3828, 2018. 5, 11
- [48] Miller, G. A. Wordnet: a lexical database for english. *Communications of the ACM*, 38(11):39–41, 1995. 32
- [49] Min, J. and Cho, M. Convolutional hough matching networks. In *Proceedings of the IEEE/CVF Conference on Computer Vision and Pattern Recognition*, pp. 2940–2950, 2021. 2, 3, 4, 18
- [50] Nauta, M., Jutte, A., Provoost, J., and Seifert, C. This looks like that, because... explaining prototypes for interpretable image recognition. In *Joint European Conference on Machine Learning and Knowledge Discovery in Databases*, pp. 441–456. Springer, 2021. 1, 11
- [51] Nauta, M., van Bree, R., and Seifert, C. Neural prototype trees for interpretable fine-grained image recognition. In *Proceedings of the IEEE/CVF Conference on Computer Vision and Pattern Recognition*, pp. 14933–14943, 2021. 1, 3, 11
- [52] Nguyen, A., Yosinski, J., and Clune, J. Deep neural networks are easily fooled: High confidence predictions for unrecognizable images. In *Proceedings of the IEEE conference on computer vision and pattern recognition*, pp. 427–436, 2015. 6
- [53] Nguyen, G., Kim, D., and Nguyen, A. The effectiveness of feature attribution methods and its correlation with automatic evaluation scores. *Advances in Neural Information Processing Systems*, 34, 2021. 1, 4, 5, 6, 8, 11
- [54] Palan, S. and Schitter, C. Prolific. ac—a subject pool for online experiments. *Journal of Behavioral and Experimental Finance*, 17:22–27, 2018. 6
- [55] Papernot, N. and McDaniel, P. Deep k-nearest neighbors: Towards confident, interpretable and robust deep learning. *arXiv preprint arXiv:1803.04765*, 2018. 1
- [56] Raghu, M., Blumer, K., Corrado, G., Kleinberg, J., Obermeyer, Z., and Mullainathan, S. The algorithmic automation problem: Prediction, triage, and human effort. *arXiv preprint arXiv:1903.12220*, 2019. 11
- [57] Ribeiro, M. T., Singh, S., and Guestrin, C. Why should i trust you?: Explaining the predictions of any classifier. In *Proceedings of the 22nd ACM SIGKDD International Conference on Knowledge Discovery and Data Mining*, pp. 1135–1144. ACM, 2016. 10
- [58] Rocco, I., Cimpoi, M., Arandjelović, R., Torii, A., Pajdla, T., and Sivic, J. Neighbourhood consensus networks. *Advances in neural information processing systems*, 31, 2018. 4
- [59] Rudin, C. Stop explaining black box machine learning models for high stakes decisions and use interpretable models instead. *Nature Machine Intelligence*, 1(5):206–215, 2019. 2, 11

- [60] Rudin, C., Chen, C., Chen, Z., Huang, H., Semenova, L., and Zhong, C. Interpretable machine learning: Fundamental principles and 10 grand challenges. *arXiv preprint arXiv:2103.11251*, 2021. 11
- [61] Russakovsky, O., Deng, J., Su, H., Krause, J., Satheesh, S., Ma, S., Huang, Z., Karpathy, A., Khosla, A., Bernstein, M., et al. Imagenet large scale visual recognition challenge. *International Journal of Computer Vision*, 115(3):211–252, 2015. 2, 7, 20
- [62] Schemmer, M., Hemmer, P., Kühn, N., Benz, C., and Satzger, G. Should i follow ai-based advice? measuring appropriate reliance in human-ai decision-making. *arXiv preprint arXiv:2204.06916*, 2022. 11
- [63] Shen, H. and Huang, T.-H. How useful are the machine-generated interpretations to general users? a human evaluation on guessing the incorrectly predicted labels. In *Proceedings of the AAAI Conference on Human Computation and Crowdsourcing*, volume 8, pp. 168–172, 2020. 5
- [64] Singh, G. and Yow, K.-C. These do not look like those: An interpretable deep learning model for image recognition. *IEEE Access*, 9:41482–41493, 2021. 1
- [65] Singla, A., Bogunovic, I., Bartók, G., Karbasi, A., and Krause, A. Near-optimally teaching the crowd to classify. In *International Conference on Machine Learning*, pp. 154–162. PMLR, 2014. 5
- [66] Stylianou, A., Souvenir, R., and Pless, R. Visualizing deep similarity networks. In *2019 IEEE winter conference on applications of computer vision (WACV)*, pp. 2029–2037. IEEE, 2019. 18
- [67] Turner, A., Kaushik, M., Huang, M.-T., and Varanasi, S. Calibrating trust in ai-assisted decision making. 9
- [68] Van Horn, G., Mac Aodha, O., Song, Y., Cui, Y., Sun, C., Shepard, A., Adam, H., Perona, P., and Belongie, S. The inaturalist species classification and detection dataset. In *Proceedings of the IEEE conference on computer vision and pattern recognition*, pp. 8769–8778, 2018. 3, 7
- [69] Wah, C., Branson, S., Welinder, P., Perona, P., and Belongie, S. The caltech-ucsd birds-200-2011 dataset. 2011. 2, 3, 7
- [70] Wang, H., Ge, S., Lipton, Z., and Xing, E. P. Learning robust global representations by penalizing local predictive power. *Advances in Neural Information Processing Systems*, 32, 2019. 2, 7, 20
- [71] Yang, X. J., Unhelkar, V. V., Li, K., and Shah, J. A. Evaluating effects of user experience and system transparency on trust in automation. In *2017 12th ACM/IEEE International Conference on Human-Robot Interaction (HRI)*, pp. 408–416. IEEE, 2017. 9
- [72] Zhang, C., Cai, Y., Lin, G., and Shen, C. Deepemd: Few-shot image classification with differentiable earth mover’s distance and structured classifiers. In *Proceedings of the IEEE/CVF conference on computer vision and pattern recognition*, pp. 12203–12213, 2020. 1, 7, 10, 11, 17
- [73] Zhang, Q., Lee, M. L., and Carter, S. You complete me: Human-ai teams and complementary expertise. In *CHI Conference on Human Factors in Computing Systems*, pp. 1–28, 2022. 11
- [74] Zhang, Y., Liao, Q. V., and Bellamy, R. K. Effect of confidence and explanation on accuracy and trust calibration in ai-assisted decision making. In *Proceedings of the 2020 Conference on Fairness, Accountability, and Transparency*, pp. 295–305, 2020. 10, 11
- [75] Zhao, W., Rao, Y., Wang, Z., Lu, J., and Zhou, J. Towards interpretable deep metric learning with structural matching. In *Proceedings of the IEEE/CVF International Conference on Computer Vision*, pp. 9887–9896, 2021. 1, 3, 4, 7, 10, 11, 17, 18

Checklist

The checklist follows the references. Please read the checklist guidelines carefully for information on how to answer these questions. For each question, change the default **[TODO]** to **[Yes]**, **[No]**, or **[N/A]**. You are strongly encouraged to include a **justification to your answer**, either by referencing the appropriate section of your paper or providing a brief inline description. For example:

- Did you include the license to the code and datasets? **[Yes]** See Section ??.
- Did you include the license to the code and datasets? **[No]** The code and the data are proprietary.
- Did you include the license to the code and datasets? **[N/A]**

Please do not modify the questions and only use the provided macros for your answers. Note that the Checklist section does not count towards the page limit. In your paper, please delete this instructions block and only keep the Checklist section heading above along with the questions/answers below.

1. For all authors...
 - (a) Do the main claims made in the abstract and introduction accurately reflect the paper’s contributions and scope? **[Yes]** . **Please see Sec. 3.**
 - (b) Did you describe the limitations of your work? **[Yes]** . **Please see Sec. 5.**
 - (c) Did you discuss any potential negative societal impacts of your work? **[N/A]** .
 - (d) Have you read the ethics review guidelines and ensured that your paper conforms to them? **[Yes]** .
2. If you are including theoretical results...
 - (a) Did you state the full set of assumptions of all theoretical results? **[Yes]** .
 - (b) Did you include complete proofs of all theoretical results? **[N/A]** .
3. If you ran experiments...
 - (a) Did you include the code, data, and instructions needed to reproduce the main experimental results (either in the supplemental material or as a URL)? **[No]** .
 - (b) Did you specify all the training details (e.g., data splits, hyperparameters, how they were chosen)? **[Yes]** . **Please see Sec. 2.**
 - (c) Did you report error bars (e.g., with respect to the random seed after running experiments multiple times)? **[Yes]** . **We reported whenever possible. See μ and σ in Table. 2.**
 - (d) Did you include the total amount of compute and the type of resources used (e.g., type of GPUs, internal cluster, or cloud provider)? **[No]** .
4. If you are using existing assets (e.g., code, data, models) or curating/releasing new assets...
 - (a) If your work uses existing assets, did you cite the creators? **[Yes]** . **We cited the authors and include the URLs.**
 - (b) Did you mention the license of the assets? **[N/A]** . **We used publicly-available datasets and code.**
 - (c) Did you include any new assets either in the supplemental material or as a URL? **[No]** .
 - (d) Did you discuss whether and how consent was obtained from people whose data you’re using/curating? **[Yes]** . **We explained to participants how their data will be used.**
 - (e) Did you discuss whether the data you are using/curating contains personally identifiable information or offensive content? **[Yes]** . **We checked and ensured that our data does not contain personally identifiable information or offensive content.**
5. If you used crowdsourcing or conducted research with human subjects...
 - (a) Did you include the full text of instructions given to participants and screenshots, if applicable? **[Yes]** . **See screenshots in Appendix D.**
 - (b) Did you describe any potential participant risks, with links to Institutional Review Board (IRB) approvals, if applicable? **[N/A]** .
 - (c) Did you include the estimated hourly wage paid to participants and the total amount spent on participant compensation? **[Yes]** . **See Sec. 2.3.4. Our rate was \$13.5/hr, higher than the Prolific recommended rate wage of \$9.60/hr.**

Appendix for: Visual correspondence-based explanations improve AI robustness and human-AI team accuracy

A Implementation details

A.1 Fine-tuning iNaturalist-pretrained ResNet-50 for CUB

To make a 200-way classifier using the ResNet-50 model from [4], we remove the 5089-way classification head and add an average pool followed by a linear feed-forward layer with 200 units. We keep all the initialization parameters unchanged and use the Adam optimizer [43] without any hyperparameter tuning. We train the new layer using the CUB training set for 200 epochs. We do not train the intermediate layers since this backbone is shared among all methods (i.e., we freeze all the convolutional layers in the ResNet-50 model). The iNaturalist-pretrained ResNet-50 model has slight difference compared to the PyTorch reference implementation [8]. The iNaturalist-pretrained ResNet-50 has 18 extra layers in the last convolutional blocks, but the spatial dimension matches the original one (i.e., $2048 \times 7 \times 7$).

A.2 Implementation details for EMD-Corr

kNN classifier We implement a vanilla kNN classifier but that operates at the deep feature space of ResNet-50. That is, given a query image Q , we sort all training-set images $\{G_i\}$ based on their distance $D(Q, G_i)$, which is the cosine distance between the two corresponding image features $f(Q)$ and $f(G_i) \in \mathbb{R}^{2048}$ at layer4 of ResNet-50, after avgpool (see [code](#)):

$$D(Q, G_i) = 1 - \frac{\langle f(Q), f(G_i) \rangle}{\|f(Q)\| \|f(G_i)\|} \quad (1)$$

where $\langle \cdot \rangle$ is the dot product, and $\|\cdot\|$ is the L_2 norm operator.

EMD-Corr classifier Similar to [75, 29], we integrate EMD into a 2-stage hierarchical image retriever. In the first stage, we select the N images having the lowest cosine distance – $\{G_i\}$ vs. the query Q by the kNN classifier. Then, we sort these N images again (a.k.a re-ranking [29]) using patch-wise similarity derived from Earth Mover Distance (EMD). In the last step, the predicted label is determined by a majority vote of top- k images’ labels like the kNN classifier, where $k \leq N$.

Our patch-wise comparison algorithm in stage 2 (shown in Fig. 3a) is different from [29, 75, 72] as the similarity of an image pair is not determined by all possible patches. Because the first stage retrieved $\{G_i\}^N$ using global features, comparing only a few most similar patches (i.e., each patch-by-patch comparison denotes a correspondence) by EMD offers benefits: (1) helping classifiers capture the distinctive image regions only (e.g., head-to-head comparison for birds); and (2) achieving human interpretability as looking at all possible pair-wise comparisons is impossible.

The most similar patches between two images Q and G – both divided into M patches – are found as a set of 2-D coordinates L containing the *highest* values in a *flow* matrix F . Let $\mathcal{Q} = \{(q_1, w_{q_1}), (q_2, w_{q_2}), \dots, (q_M, w_{q_M})\}$ and $\mathcal{G} = \{(g_1, w_{g_1}), (g_2, w_{g_2}), \dots, (g_M, w_{g_M})\}$ denote two sets of non-overlapping image patches, g_i and g_j are the patch embeddings; and w_{q_i} and w_{g_j} are the

corresponding importance assigned by a feature weighting algorithm (e.g., Cross Correlation used in [75]). We derive $\mathbf{F} = (f_{ij}) \in \mathbb{R}^{M \times M}$ by minimizing the *transport plan cost* in Eq. 2.

$$\text{Cost}(Q, G, \mathbf{F}) = \sum_{i=1}^M \sum_{j=1}^M d_{ij} f_{ij} \quad (2)$$

where $f_{ij} \geq 0$ and $\sum_{j=1}^M \sum_{i=1}^M f_{ij} = 1$. We use Eq. 1 to compute the ground distance d_{ij} and run the Sinkhorn algorithm [21] for 100 iterations to seek the *optimal transport plan* \mathbf{F} . To assign importance weights (i.e., w_{q_i} and w_{g_j}), we use cross-correlation (CC) maps from [66].

Finally, using \mathbf{F} and D from Eq. 1, the EMD distance between Q and G is computed by Eq. 3. Since we are interested in patch-wise comparison, the features used in stage 2 of Q and G are layer4 from [8]. Our EMD-Corr classifier’s stage 2 solely relies on EMD distance for re-ranking instead of mixing EMD and cosine distance like [75, 29].

$$d_{\text{EMD}}(D, \mathbf{F}) = \sum_{(i,j) \in L} d_{ij} f_{ij} \quad (3)$$

A.3 Implementation details for CHM-Corr classifier

Similar to the EMD-Corr classifier, this classifier also consists of 2 stages – selecting N most similar images to the query Q by the kNN classifier, followed by a correspondence-based re-ranking algorithm. For re-ranking, we propose to use a Convolutional Hough Matching network (CHM) [49] to first infer semantic correspondences between Q and G , then calculate the similarity score between these two images based on a subset of correspondences.

The re-ranking algorithm starts with dividing both Q and G into M patches, resulting in two set of $\mathcal{Q} = \{q_1, q_2, \dots, q_M\}$ and $\mathcal{G} = \{g_1, g_2, \dots, g_M\}$ image patches. To find the semantic correspondences between two images, we make use of the CHM network to transfer keypoints from the query image Q to image G .

The CHM network extracts features from multiple layers of a ResNet-101 network to construct a set of multi-scale features $\{(\mathbf{F}_Q, \mathbf{F}_G)\}_{s=1}^S$. It will construct a correlation tensor by comparing all possible pairs in the feature space of two images. Lastly, using the correlation tensor, the CHM network performs Hough voting in the space of translation and scale to find candidate matches, resulting in a set of M correspondence (q_i, g_j) pairs. After finding visual correspondence between two images, we assign an importance weight $w_{i,j}$ for the pair (q_i, g_j) using cross-correlation maps from [66]. Finally, the distance between Q and G is the average distance between 5 patch pairs with the lowest cosine distance.

We use the reference implementation of the Convolutional Hough Matching Network pretrained on the PF-Pascal Dataset [30]. There are three variations of CHM networks depending on parameters sharing strategy, i.e., psi, iso, and full. Our ablation study (Appendix B.3) shows similar performance on a 5K subset of ImageNet dataset. We select psi with a threshold of $T = 0.55$ for the CHM-Corr classifier.

The CHM network requires a set of initial keypoints on the source image, i.e., a set of keypoint on the query image Q . Although some datasets come with this annotation information, generally, this information is not available. To have a comparable classifier with our EMD-Corr classifier, we discretize an image into a 7×7 grid, resulting in 49 non-overlapping patches. For each patch, we pick a point at its center.

For assigning importance weight $w_{i,j}$ to (q_i, g_j) pair, we first calculate the cross-correlation map between the two images Q and G . Calculating a cross-correlation map using the last convolutional layer of the ResNet-50 model will result in two 7×7 maps for each Q and G . For assigning importance weights, we binarize the cross-correlation for Q , using a threshold of $T = 0.55$, i.e., we zero out all pairs in the non-salient part according to Q , by setting their importance weights to 0, and for the remaining patches, we set the weights to 1.

After removing non-salient patch pairs in the last stage, we calculate the cosine similarity between pair (q_i, g_j) using the corresponding feature volume in the last convolutional layer of the ResNet-50 model. The similarity score is the average similarity between top 5 pairs with the highest cosine similarity.

A.4 Generating Adversarial Patch dataset

Brown et al. [15] generated a *universal* adversarial patch to fool image classifiers to recognize everything as toaster. This patch misleads models' attention, overly looking at the most salient item while ignoring the remaining pixels. We apply this attack on ImageNet validation set, resulting in 50K Adversarial Patch images of 240×240 px. The patches are circles with the size of 5% the input image, targeting on ResNet-50 [31] classifying everything as toaster with target confidence of 90%. The maximum attack iteration for each sample is 500. We only train to optimize the adversarial patch on ImageNet validation set for one epoch and save the immediate samples for the dataset. We adapt the code from [2] and make minor modifications.

To obtain our Adversarial Patch dataset, from the [main repository](#), you can run the below command to generate the dataset or download the dataset [here](#).

```
cd datasets/adversarial-patch/  
python make_patch.py --cuda --epochs 1 --patch_size 0.05 --max_count 500  
--netClassifier resnet50 --patch_type circle --train_size 50000  
--test_size 0 --image_size 240 --outf output_imgs
```

B Ablation study and small-scale experiments on ImageNet OODs

B.1 Different hyperparameters for EMD

Table A1: Accuracy of the EMD-Corr classifier with different EMD Hyperparameters (%)

Datasets	Number of Images	Cross Correlation Corrs-Num= 5 $k = 20$	Cross Correlation Corrs-Num= 49×49 $k = 20$	Uniform Corrs-Num= 5 $k = 20$
ImageNet 2012	50,000	74.93	74.59	74.47
CUB (iNaturalist ResNet)	5,794	84.98	85.42	79.72
CUB (ImageNet ResNet)	5,794	n/a	59.44	53.47

B.2 Performance of classifiers on a 5K subset of different datasets

Table A2 contains details about the performance of different classifiers on a 5K subset of various OOD datasets.

Table A2: Performance of classifiers on 5K subsets of various OOD datasets – (Accuracy %)

Datasets	ResNet-50	kNN	EMD-Corr	CHM-Corr
ImageNet [61]	75.00	74.62	74.66	74.52
ImageNet-R [35]	35.68	34.60	35.66	36.18
ObjectNet [13]	36.54	34.80	36.56	35.60
ImageNet Sketch [70]	23.84	23.92	24.40	25.28
ImageNet-A [36]	0.00	0.32	0.50	0.46
DAMageNet [18]	6.38	8.92	9.72	9.06
ImageNet-C Gaussian noise (Level 1) [34]	59.56	59.62	59.70	59.62
ImageNet-C Gaussian blur (Level 1) [34]	66.12	65.68	65.68	65.68

B.3 Different weights for CHM

Table A3: Accuracy of the CHM-Corr classifier on a 5K subset of ImageNet [61] with different CHM parameters (%)

Method	Threshold							
	0.2	0.3	0.4	0.5	0.55	0.6	0.7	0.8
PSI	74.26	74.36	74.36	74.26	74.52	74.38	74.44	73.78
ISO	74	74.04	74	74.18	74.24	74.28	74.1	73.76
FULL	74.62	74.62	74.48	74.64	74.4	74.44	74.56	74.02

C Sample explanations

This section contains sample visualization for kNN, EMD-Corr, and CHM-Corr classifiers.

C.1 kNN



Figure A1: A sample explanation of the kNN classifier when classifying a chihuahua image.

C.2 EMD-NN



Figure A2: A sample EMD-NN explanation of the EMD-Corr classifier when classifying a great grey owl image. EMD-NN shows only nearest neighbors after re-ranking.

C.3 EMD-Corr

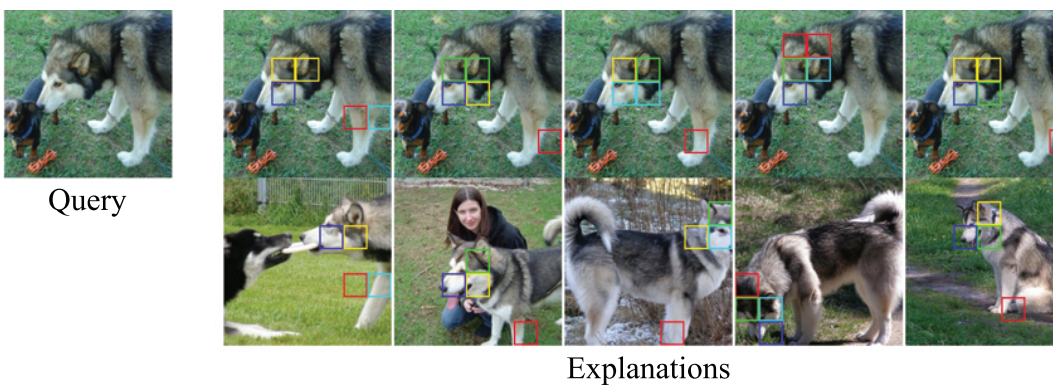


Figure A3: A sample explanation of the EMD-Corr classifier when classifying a malamute image.

C.4 CHM-NN



Figure A4: A sample CHM-NN explanation of the CHM-Corr classifier when classifying a vacuum image. CHM-NN only shows nearest neighbors after re-ranking.

C.5 CHM-Corr

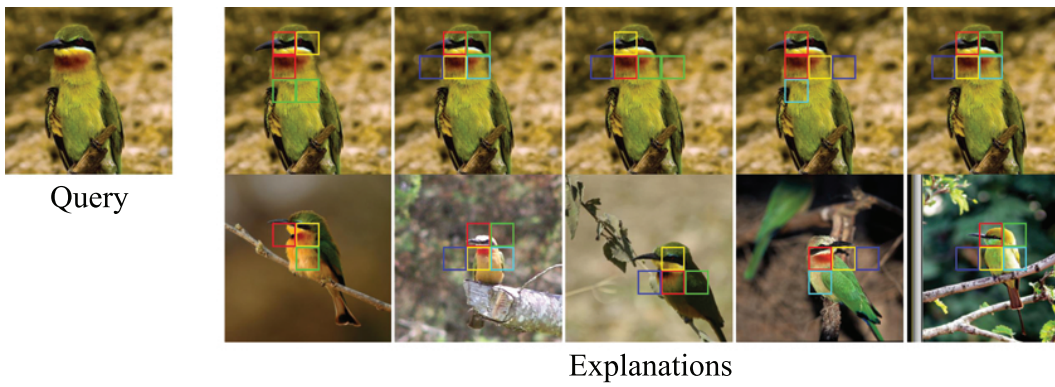


Figure A5: A sample explanation of the CHM-Corr classifier when classifying a bee eater image.

D Sample screens and training examples for human studies

D.1 Sample screens from human studies

Have you ever seen a **steel drum** before?

No

steel drum: a concave percussion instrument made from the metal top of an oil drum



Continue

(a) ImageNet studies



Red-faced cormorant

Continue

(b) CUB studies

Figure A6: In ImageNet-ReaL experiments, before each trial, where users are asked if the query image belongs to the top-1 class c (here, **steel drum**), we show three representative images from c along with a 1-sentence WordNet description (a). Instead of showing 3 images, in CUB experiments, we show 6 images from the top-1 class (here, Red-faced Cormorant) to help users better recognize the distinct features of each bird.



Figure A7: A sample screenshot from a human study of EMD-Corr users. Each user is provided with (1) the query image; (2) AI top-1 predicted label and confidence score; and (3) an explanation, here the visual correspondence-based explanations of EMD-Corr. They are asked to provide a Yes/No answer whether the query is an image of junco.

D.2 Sample groundtruth cases used in the Validation phase of our CUB human studies

Below are example cases that we manually choose to be “groundtruth” in order to control for user quality during the validation phase.

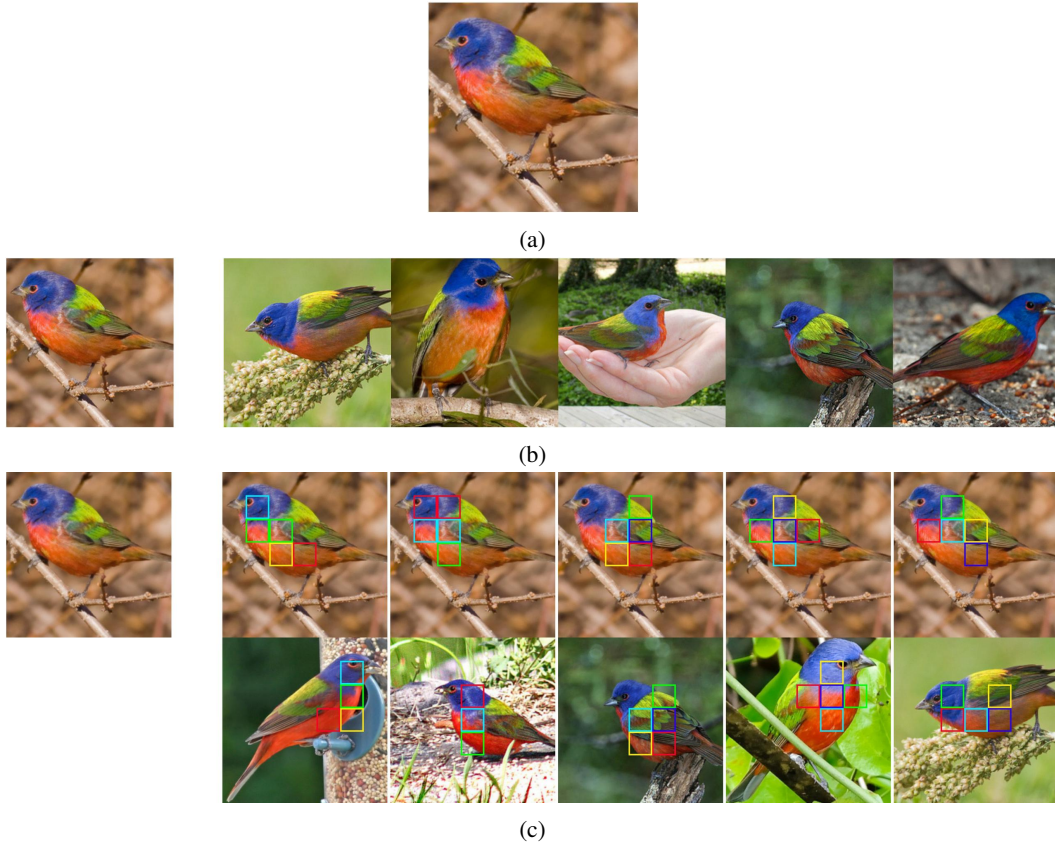


Figure A8: A **groundtruth Yes** validation sample in a CUB study. That is, users are expected to select Yes when being presented with these explanations. The bird is Painted Bunting.

(a) ResNet-50—no explanations provided.

(b) kNN nearest-neighbor explanation.

(c) EMD-Corr explanation.

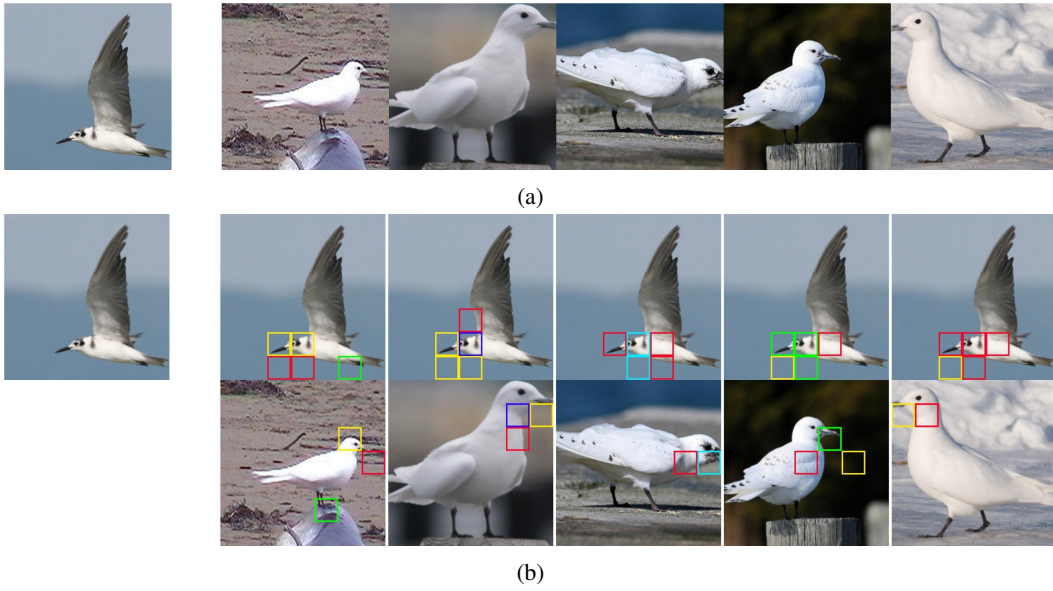


Figure A9: A **groundtruth No** validation sample in a CUB study. That is, users are expected to select No when being presented with these explanations. The bird is Black Tern.
(a) EMD-NN explanation.
(b) EMD-Corr explanation.

E Human-AI team performance analysis

This section provides more details about AI and team performance.

E.1 Defining the difficulty level of queries

To further understand the performance of the classifiers in our study, we categorize each query image into Easy, Medium, and Hard categories based on the model’s confidence score and the correctness of the top-1 label (see Table A4). This breakdown allows us to analyze model and user behaviors in a specific level of difficulty.

Table A4: Difficulty levels

	Easy	Medium	Hard
AI is Correct	confidence $\in [0, 0.35)$	confidence $\in [0.35, 0.75)$	confidence $\in [0.75, 1)$
AI is Wrong	confidence $\in [0.75, 1)$	confidence $\in [0.35, 0.75)$	confidence $\in [0, 0.35)$

E.2 The acceptance and rejection ratios

In Table A5 we provide details about whether users accepted or rejected AI's decisions for each type of classifier.

Table A5: The frequency of users accepting or rejecting AI's decision per classifier (%).

Method	ImageNet-ReaL		CUB	
	Accept	Reject	Accept	Reject
ResNet-50	60.44	39.56	74.28	25.72
kNN	69.60	30.40	81.53	18.47
EMD-Corr	64.92	35.08	67.30	32.70
CHM-Corr	67.51	32.49	66.27	33.73
EMD-NN	67.49	32.51	78.76	21.24
CHM-NN	68.94	31.06	76.94	23.06

Table A6 shows the ratio of accept and reject based on the difficulty level described in Sec. E.1.

Table A6: The ratio of users accepting or rejecting AI's decision per difficulty level (%)

Difficulty Level	ImageNet-ReaL		CUB	
	Accept	Reject	Accept	Reject
Easy	72.7	27.3	82.75	17.25
Medium	58.42	41.58	66.43	33.57
Hard	62.38	37.62	78.34	21.66

E.3 Time performance of users

Fig. A10 shows the average time distribution to finish each trail per method.

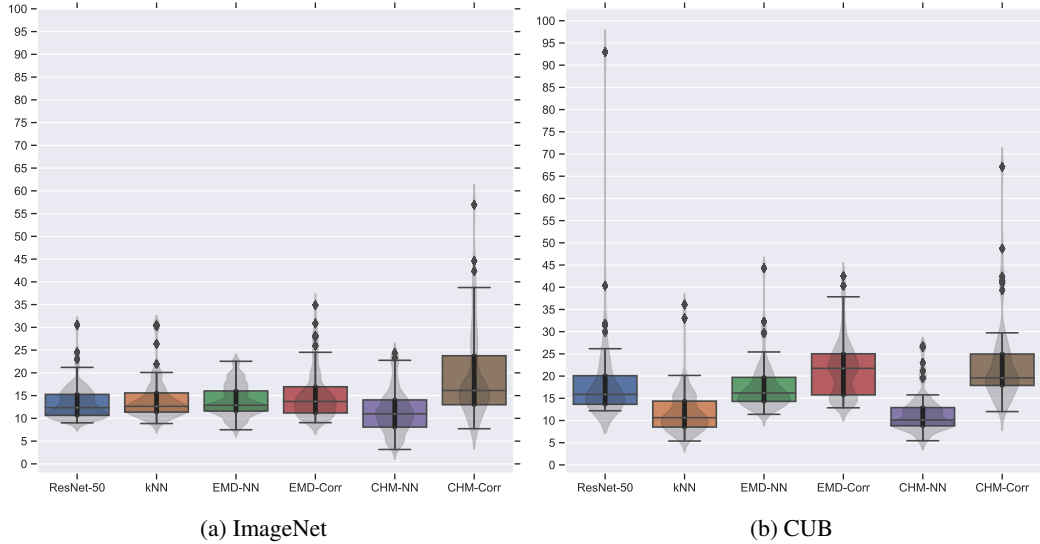


Figure A10: Distribution of the average time taken for each trial (Seconds)

E.4 Human performance analysis based on AI correctness

Figure A11 shows the breakdown of user accuracy based on the correctness of AI predictions on ImageNet-Real and CUB datasets.

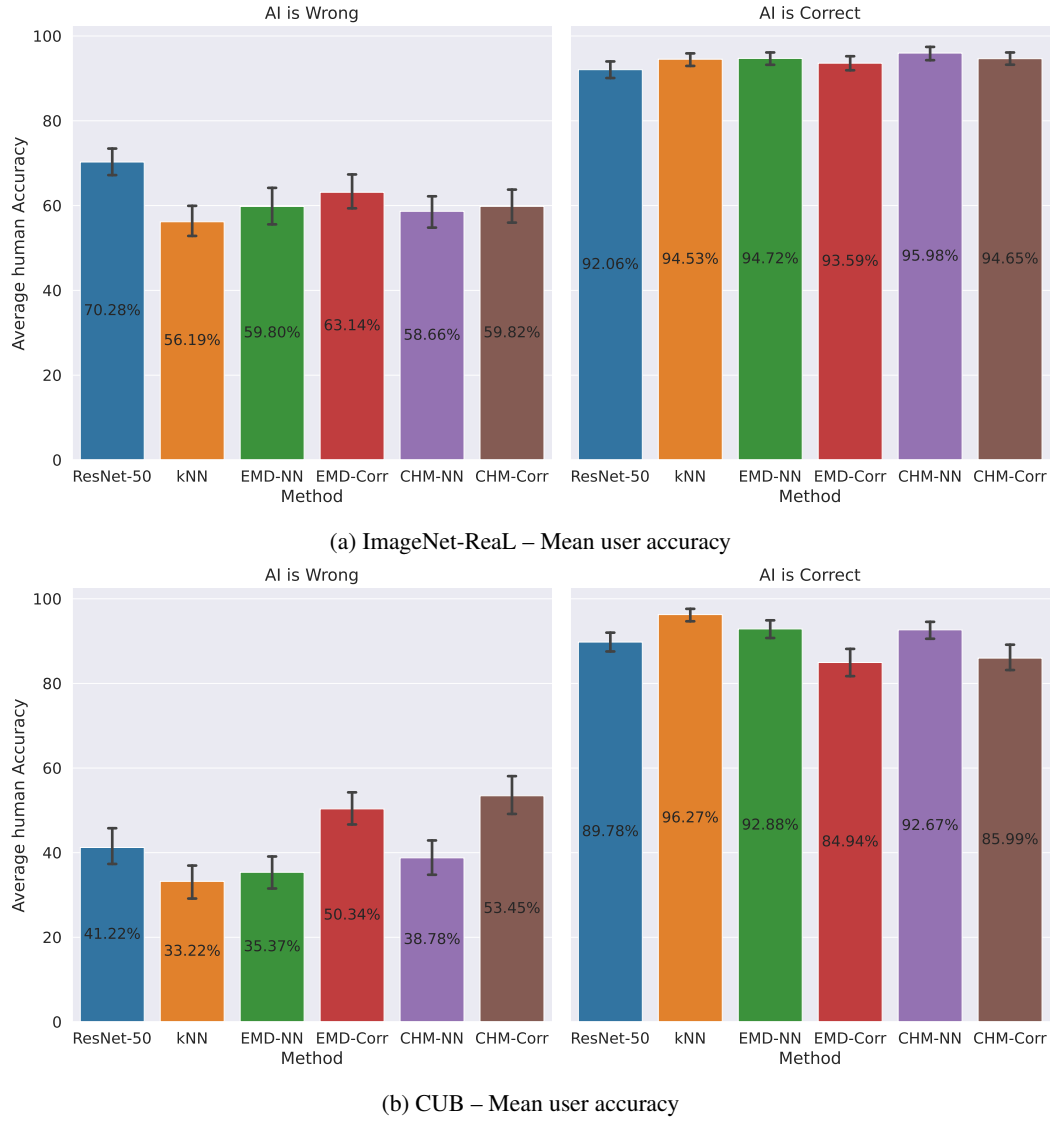
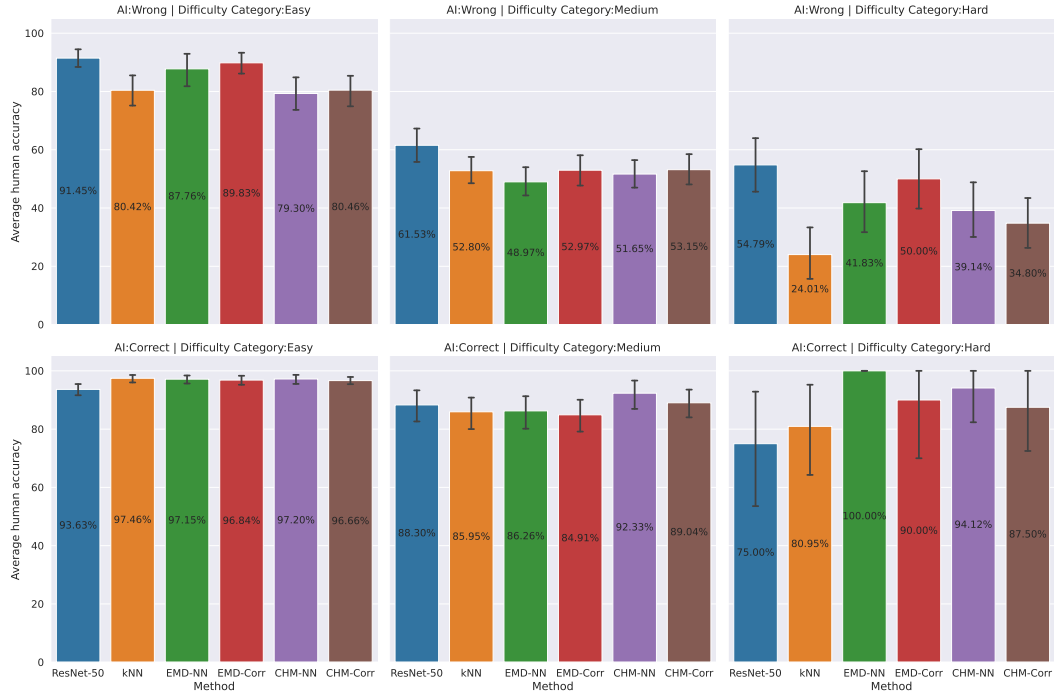


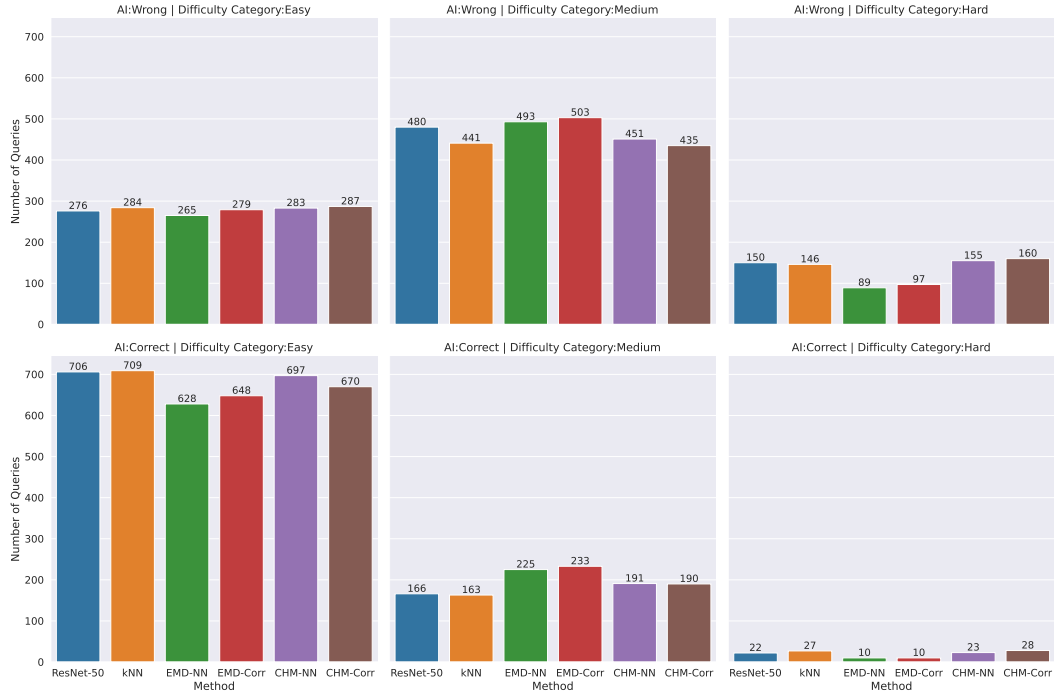
Figure A11: The breakdown of human performance by AI correctness

E.5 Human performance analysis based on the difficulty of the query

In this section, we calculate the average user accuracy based on the difficulty level of the query (Described in Sec E.1) and the correctness of AI's prediction.

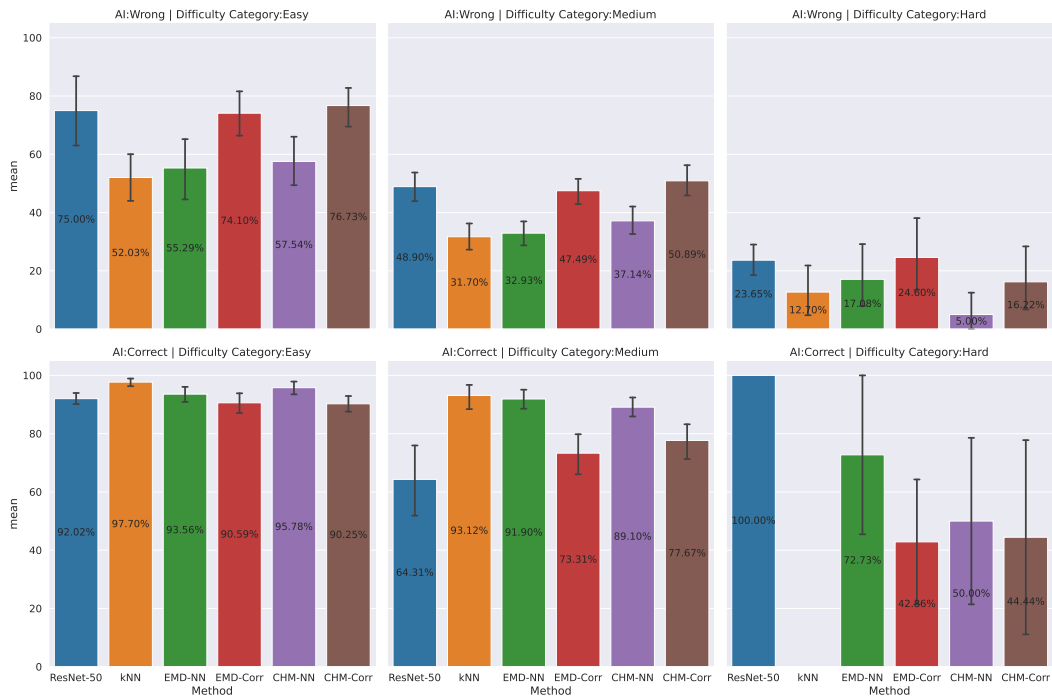


(a) Mean user accuracy

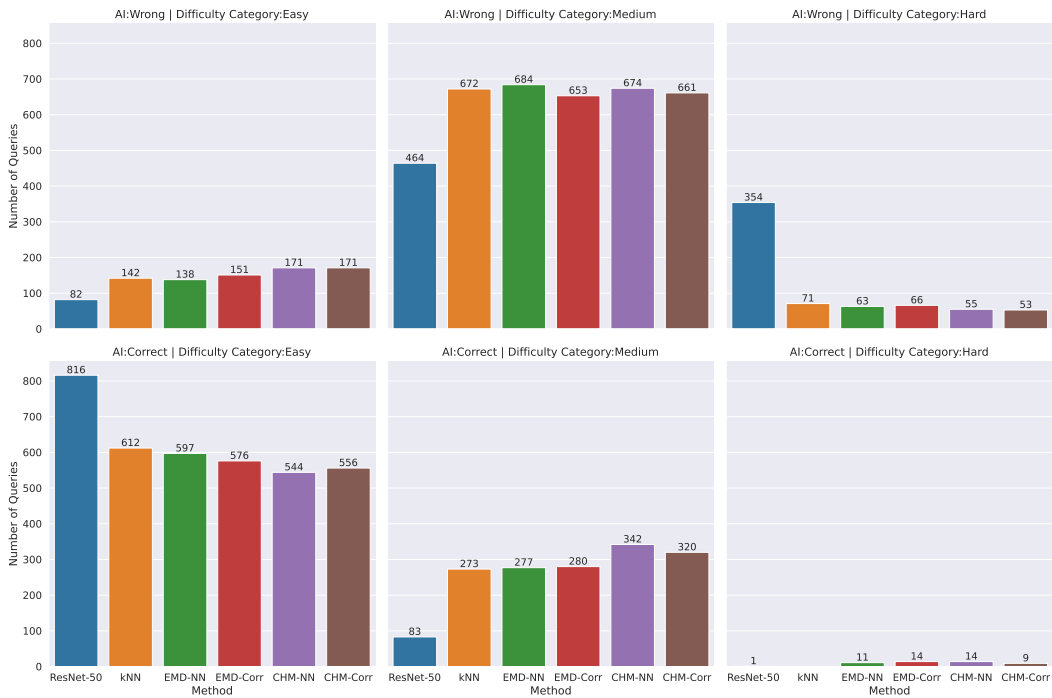


(b) Number of queries

Figure A12: ImageNet – The breakdown of the human performance by ‘Difficulty Level’ and ‘AI Correctness’



(a) Mean user accuracy



(b) Number of queries

Figure A13: CUB – The breakdown of the human performance by ‘Difficulty Level’ and ‘AI Correctness’

E.6 Analysis of Hard images for humans in the ImageNet task

This section provides the analysis to understand what kind of queries are hard for humans, i.e., for what types of images users can not correctly accept or reject the AI’s decision. To this end, we filter the queries with a mean user’s accuracy of 0.25 or below. Figure A14 shows the distribution of Hard images for humans based on the classifier and the classifier’s correctness.

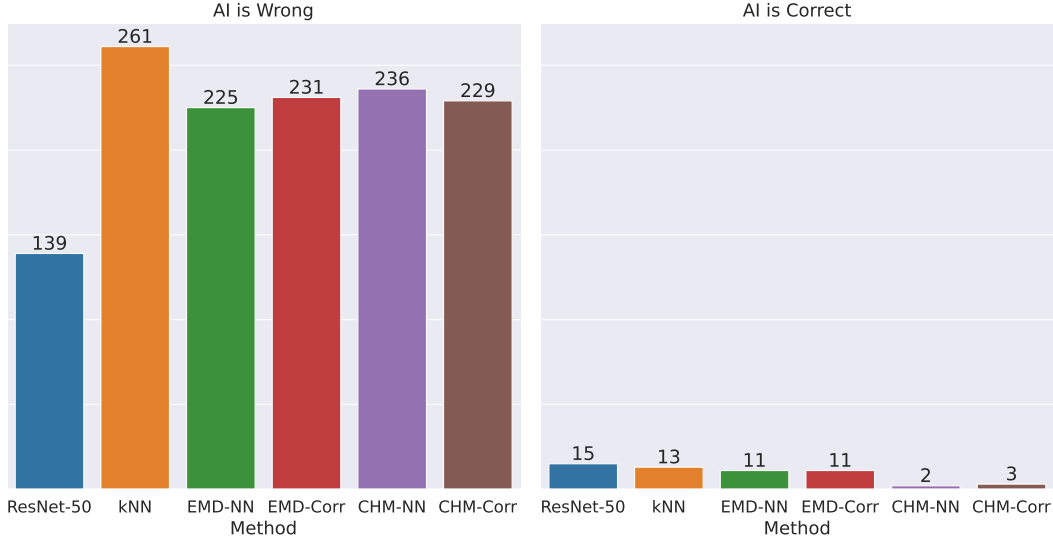


Figure A14: Number of confusing queries per classifier

To better understand what types of images are more challenging for humans, we automatically create supergroups for ImageNet class members. All 1,000 classes of ImageNet are a subgroup of `entity - n00001740` class in the WordNet glossary [48]. To create groups with uniform sizes, we start from the `entity` root node and break up each class to its sub-classes recursively; in each iteration, we pick the supergroup with the largest number of classes. Here we report the parent class of queries after 12 iterations and for queries with only one ImageNet ReaL label. Using this automated procedure, we can see that the majority of hard images for humans fall into the `carnivore` category, which is a supergroup for cats, lions, dogs, wolves, etc. Details about each parent class and its ImageNet class members can be found in Table A7.

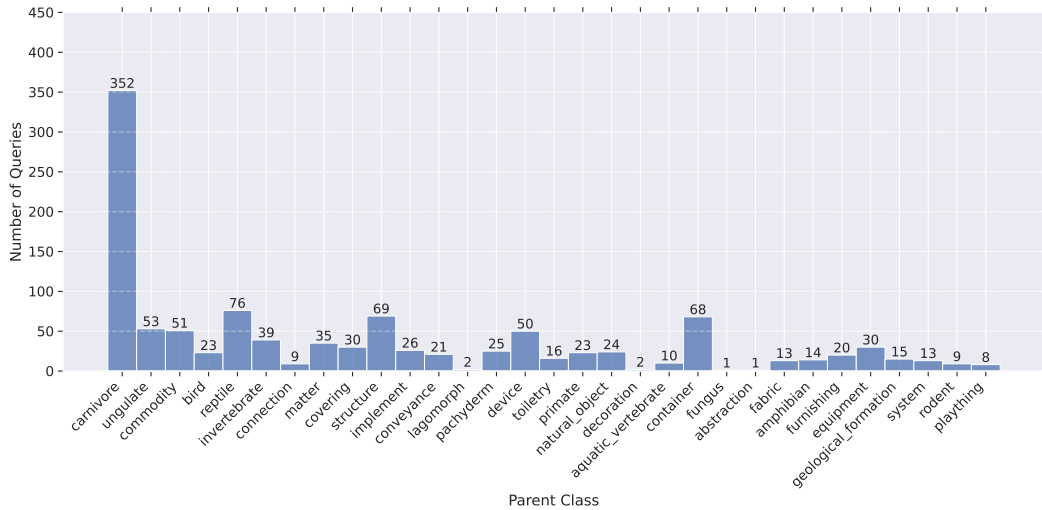


Figure A15: Parent class of confusing queries

Table A7: Parent classes of Hard queries for humans and their ImageNet class members.

Parent Class	ImageNet Class Members
Abstraction	Street Sign
Amphibian	Axolotl, European Fire Salamander, Tree Frog
Aquatic Vertebrate	Goldfish
Bird	American Egret, Bulbul, Cock, Oystercatcher, Red-Backed Sandpiper, Ruffed Grouse
Carnivore	Beagle, Black-And-Tan Coonhound, Black-Footed Ferret, Bloodhound, Bluetick, Border Terrier, Bouvier Des Flandres, Bull Mastiff, Collie, Coyote, Curly-Coated Retriever, English Foxhound, English Springer, Entlebucher, Eskimo Dog, Flat-Coated Retriever, French Bulldog, German Short-Haired Pointer, Great Dane, Great Pyrenees, Greater Swiss Mountain Dog, Irish Water Spaniel, Kelpie, Lakeland Terrier, Lhasa, Malamute, Miniature Poodle, Norfolk Terrier, Otter, Pembroke, Polecat, Redbone, Rhodesian Ridgeback, Rottweiler, Schipperke, Scotch Terrier, Scottish Deerhound, Sealyham Terrier, Shetland Sheepdog, Siberian Husky, Staffordshire Bullterrier, Standard Poodle, Standard Schnauzer, Tabby, Tibetan Terrier, Tiger Cat, Toy Poodle, Vizsla, Welsh Springer Spaniel, Yorkshire Terrier
Commodity	Abaya, Academic Gown, Dishwasher, Dutch Oven, Espresso Maker, Microwave, Military Uniform, Miniskirt, Washer
Connection	Chain
Container	Ambulance, Cassette, Envelope, Pitcher, Purse, Shopping Basket, Soap Dispenser, Soup Bowl, Tank, Wallet, Washbasin, Whiskey Jug
Conveyance	Dogsled, Schooner, Stretcher, Trolleybus, Yawl
Covering	Dome, Doormat, Pickelhaube, Prayer Rug, Scabbard, Shower Curtain
Decoration	Necklace
Device	Analog Clock, Car Wheel, Cello, Combination Lock, Padlock, Projectile, Radiator, Upright, Wall Clock
Equipment	Balance Beam, Cd Player, Dumbbell, Horizontal Bar, Monitor, Polaroid Camera
Fabric	Wool
Fungus	Hen-Of-The-Woods
Furnishing	Cradle, Crib, Desk, Entertainment Center
Geological Formation	Coral Reef, Lakeside, Seashore
Implement	Ballpoint, Plow, Plunger, Quill, Teapot
Invertebrate	Barn Spider, Bee, Cricket, Damselfly, Dragonfly, Dungeness Crab, Long-Horned Beetle, Mantis, Sea Slug, Snail, Sulphur Butterfly
Lagomorph	Wood Rabbit
Matter	Artichoke, Bell Pepper, Cheeseburger, Cucumber, Hay, Plate, Pretzel
Natural Object	Banana, Corn, Lemon, Sandbar
Pachyderm	African Elephant, Indian Elephant
Plaything	Teddy
Primate	Gibbon, Gorilla, Langur, Siamang, Titi
Reptile	African Crocodile, Alligator Lizard, American Chameleon, Banded Gecko, Boa Constrictor, Frilled Lizard, Green Mamba, Green Snake, Mud Turtle, Night Snake, Rock Python, Terrapin
Rodent	Beaver
Structure	Bakery, Bannister, Church, Cliff Dwelling, Dam, Dock, Grocery Store, Megalith, Plate Rack, Stupa, Totem Pole
System	Radio
Toiletry	Hair Spray, Lotion, Sunscreen
Ungulate	Bighorn, Bison, Hog, Impala, Llama, Water Buffalo, Wild Boar

E.7 Analysis of Hard images for humans in the bird classification task

Similar to the analysis we conducted for ImageNet in Sec.E.6, here we analyze the confusing bird types for humans. Here we filter queries with mean user accuracy below 0.25. Figure A16 shows the distribution of the most challenging samples for humans based on different classifiers' correctness.

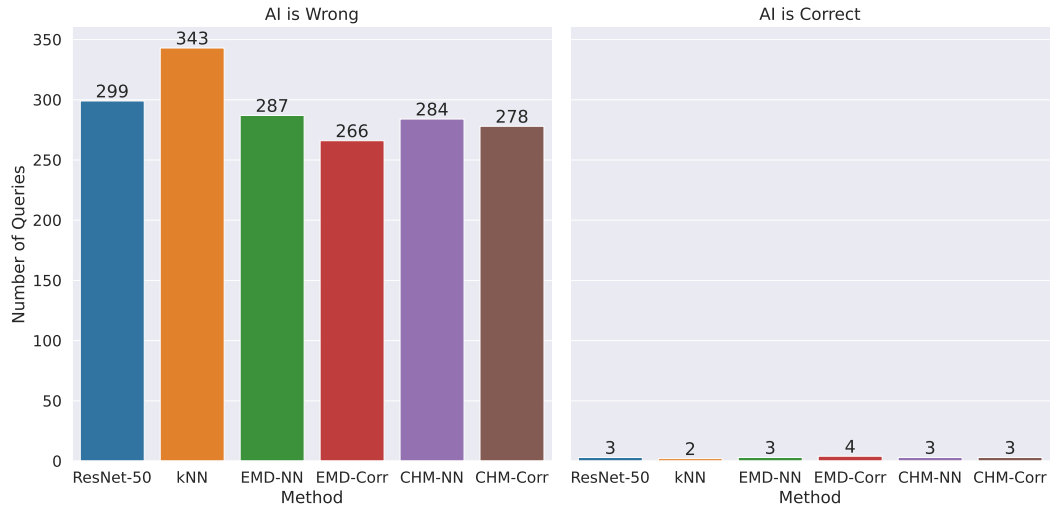


Figure A16: Number of confusing queries per classifier

Table A8 shows top 5 confusing bird types for human users. Each row in this table shows how many users failed to reject AI's prediction when providing different kinds of explanations.

Table A8: Top-5 confusing bird types for humans per classifier

Classifier	Ground Truth	Confused with	Users
ResNet-50	Forsters Tern	Common Tern	17
	Great Grey Shrike	Loggerhead Shrike	10
	Nelson Sharp Tailed Sparrow	Le Conte Sparrow	8
	Acadian Flycatcher	Least Flycatcher	7
	American Crow	Common Raven	7
kNN	California Gull	Western Gull	21
	Elegant Tern	Caspian Tern	13
	Fish Crow	American Crow	12
	Rusty Blackbird	Brewer Blackbird	11
	Acadian Flycatcher	Yellow Bellied Flycatcher	10
EMD-NN	California Gull	Western Gull	15
	Common Tern	Artic Tern	12
	Nelson Sharp Tailed Sparrow	Savannah Sparrow	8
	Acadian Flycatcher	Yellow Bellied Flycatcher	8
	Yellow Bellied Flycatcher	Acadian Flycatcher	8
EMD-Corr	California Gull	Western Gull	15
	Common Tern	Artic Tern	12
	Nelson Sharp Tailed Sparrow	Savannah Sparrow	8
	Acadian Flycatcher	Yellow Bellied Flycatcher	8
	Yellow Bellied Flycatcher	Acadian Flycatcher	8
CHM-NN	Great Grey Shrike	Loggerhead Shrike	19
	Le Conte Sparrow	Nelson Sharp Tailed Sparrow	15
	California Gull	Western Gull	15
	Louisiana Waterthrush	Northern Waterthrush	12
	Horned Grebe	Eared Grebe	9
CHM-Corr	Great Grey Shrike	Loggerhead Shrike	20
	Horned Grebe	Eared Grebe	15
	California Gull	Western Gull	15
	Louisiana Waterthrush	Northern Waterthrush	13
	Le Conte Sparrow	Nelson Sharp Tailed Sparrow	13

E.8 Accepting AI's wrong decision

This section shows samples for which users incorrectly accepted the incorrect AI prediction.

E.8.1 Accepting the wrong kNN Classifier's prediction

Query: ILSVRC2012_val_00027135.JPEG

kNN Prediction: malamute

Number of Users: 3

Mean Accuracy: 0.0

Real GT(s): fur coat, eskimo dog



Query: ILSVRC2012_val_00006190.JPEG

kNN Prediction: magnetic compass

Number of Users: 3

Mean Accuracy: 0.0

Real GT(s): analog clock



Query: ILSVRC2012_val_00019353.JPEG

kNN Prediction: rottweiler

Number of Users: 4

Mean Accuracy: 0.0

Real GT(s): black-and-tan coonhound

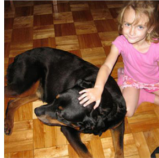


Figure A17: Accepting the wrong kNN prediction due to confusing explanations

Query: ILSVRC2012_val_00045078.JPEG

kNN Prediction: stove

Number of Users: 4

Mean Accuracy: 0.0

Real GT(s): washer



Query: ILSVRC2012_val_00027335.JPEG

kNN Prediction: cartoon

Number of Users: 3

Mean Accuracy: 0.0

Real GT(s): artichoke



Query: ILSVRC2012_val_00021555.JPEG

kNN Prediction: bookshop

Number of Users: 3

Mean Accuracy: 0.0

Real GT(s): library, bookcase



Figure A18: Accepting the wrong kNN prediction due to poor ImageNet ReaL labeling

E.8.2 Accepting the wrong EMD-NN Classifier's prediction

Query: ILSVRC2012_val_00031321.JPEG
EMD Prediction: custard apple

Number of Users: 3
Mean Accuracy: 0.0

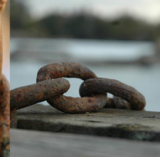
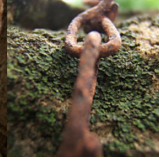
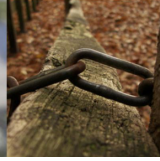
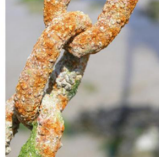
Real GT(s): snail



Query: ILSVRC2012_val_00037616.JPEG
EMD Prediction: chain

Number of Users: 3
Mean Accuracy: 0.0

Real GT(s): knot



Query: ILSVRC2012_val_00032466.JPEG
EMD Prediction: miniature poodle

Number of Users: 2
Mean Accuracy: 0.0

Real GT(s): standard poodle

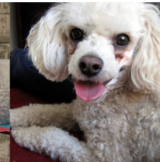
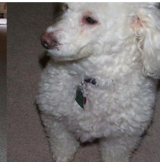
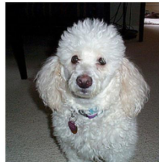
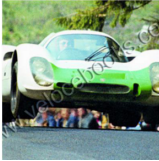


Figure A19: Accepting the wrong EMD-NN prediction due to confusing explanations

Query: ILSVRC2012_val_00046201.JPEG
EMD Prediction: racer

Number of Users: 2
Mean Accuracy: 0.0

Real GT(s): sports car, car wheel



Query: ILSVRC2012_val_00047182.JPEG
EMD Prediction: cd player

Number of Users: 3
Mean Accuracy: 0.0

Real GT(s): radio



Query: ILSVRC2012_val_00018221.JPEG
EMD Prediction: notebook

Number of Users: 4
Mean Accuracy: 0.0

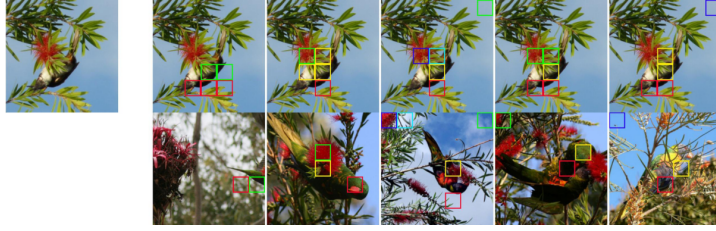
Real GT(s): laptop, computer keyboard



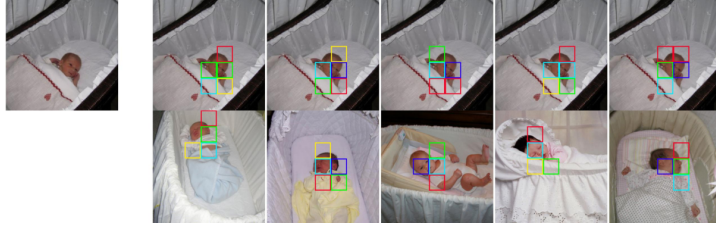
Figure A20: Accepting wrong EMD-NN prediction due to 'Bad Labels'

E.8.3 Accepting the wrong EMD-Corr Classifier's prediction

Query: ILSVRC2012_val_00007263.JPEG
 EMD Prediction: lorikeet
 Number of Users: 2
 Mean Accuracy: 0.0
 Real GT(s): bulbul



Query: ILSVRC2012_val_00015206.JPEG
 EMD Prediction: bassinet
 Number of Users: 4
 Mean Accuracy: 0.0
 Real GT(s): cradle



Query: ILSVRC2012_val_00033233.JPEG
 EMD Prediction: walker hound
 Number of Users: 4
 Mean Accuracy: 0.0
 Real GT(s): beagle

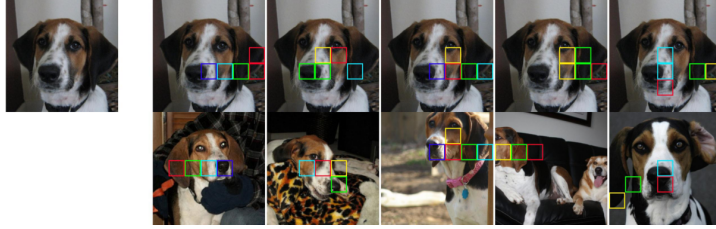
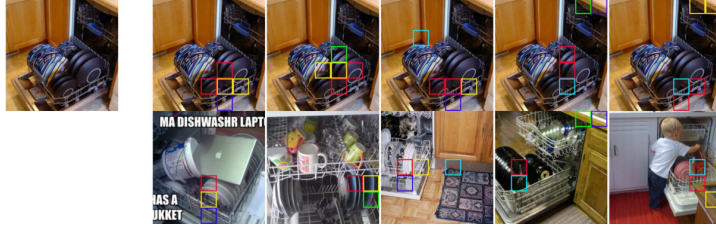
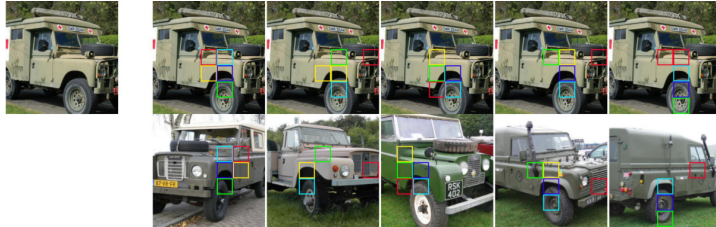


Figure A21: Accepting wrong EMD-Corr prediction due to confusing explanations

Query: ILSVRC2012_val_00019084.JPEG
 EMD Prediction: dishwasher
 Number of Users: 4
 Mean Accuracy: 0.0
 Real GT(s): plate rack



Query: ILSVRC2012_val_00025990.JPEG
 EMD Prediction: jeep
 Number of Users: 3
 Mean Accuracy: 0.0
 Real GT(s): ambulance



Query: ILSVRC2012_val_00017102.JPEG
 EMD Prediction: seashore
 Number of Users: 2
 Mean Accuracy: 0.0
 Real GT(s): sandbar

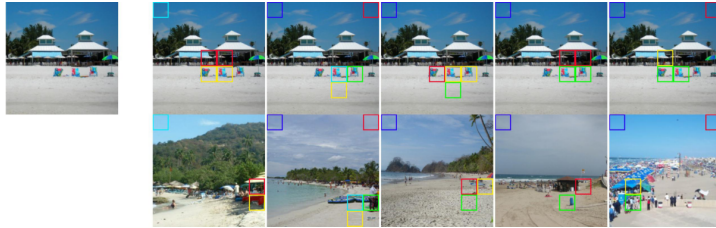


Figure A22: Accepting wrong EMD-Corr prediction due to poor ImageNet Real labeling

E.8.4 Accepting the wrong CHM-NN Classifier's prediction

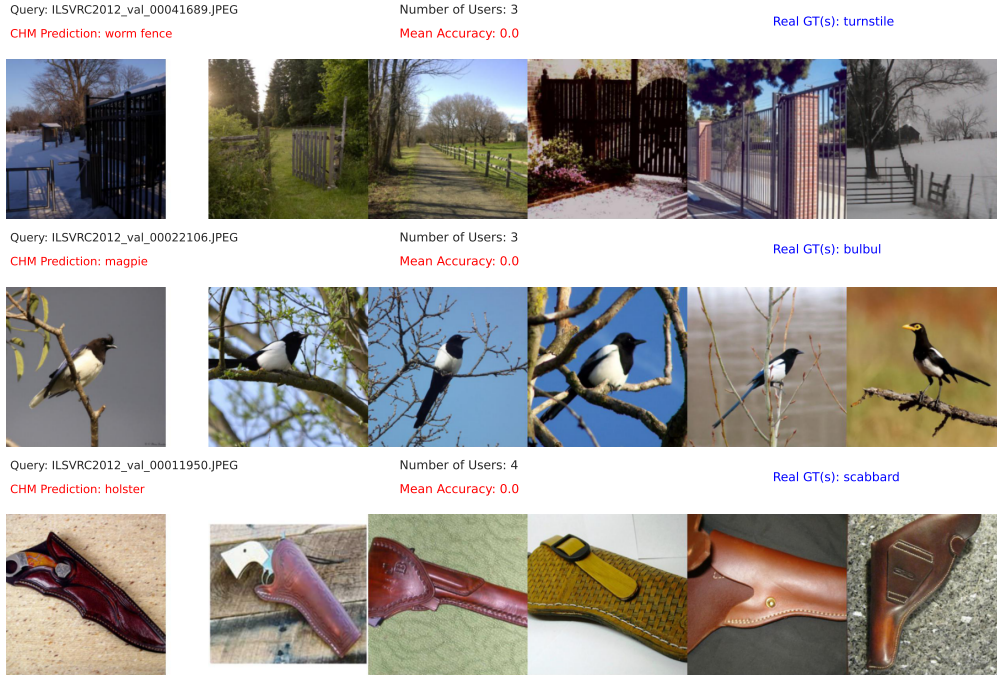


Figure A23: Accepting wrong CHM-NN prediction due to confusing explanations

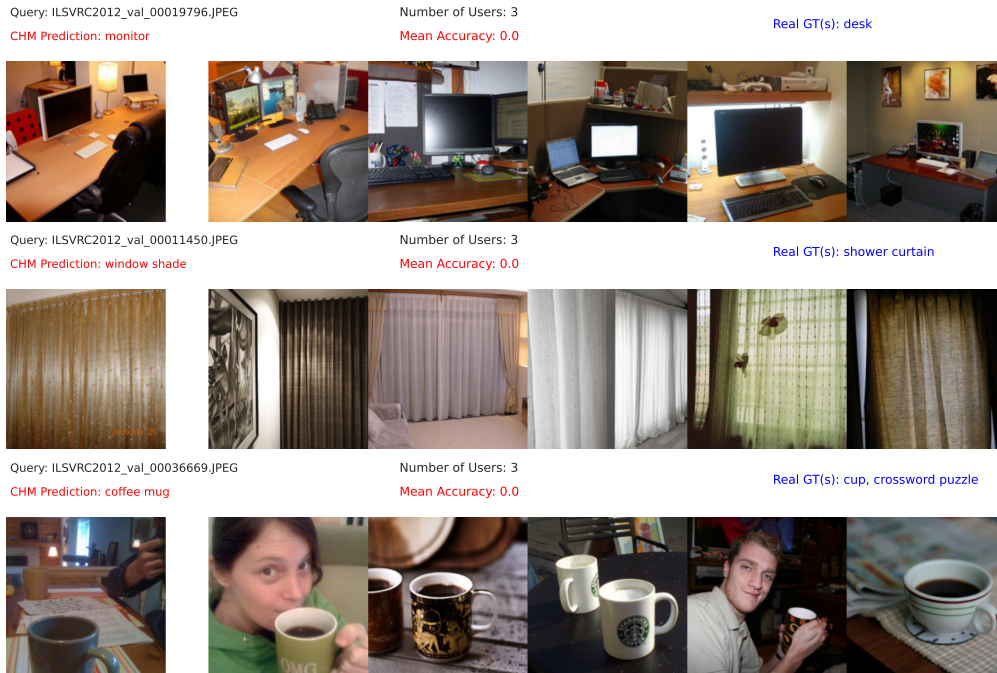
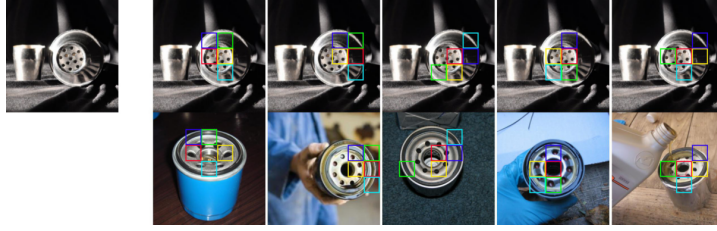


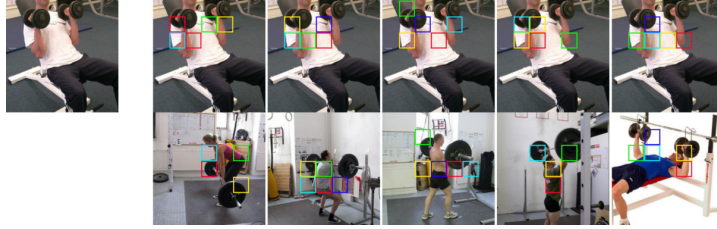
Figure A24: Accepting wrong CHM-NN prediction due to poor ImageNet Real labeling

E.8.5 Accepting the wrong CHM-Corr Classifier’s prediction

Query: ILSVRC2012_val_00002666.JPEG
 CHM Prediction: oil filter
 Number of Users: 3
 Mean Accuracy: 0.0
 Real GT(s): saltshaker



Query: ILSVRC2012_val_00026198.JPEG
 CHM Prediction: barbell
 Number of Users: 3
 Mean Accuracy: 0.0
 Real GT(s): dumbbell

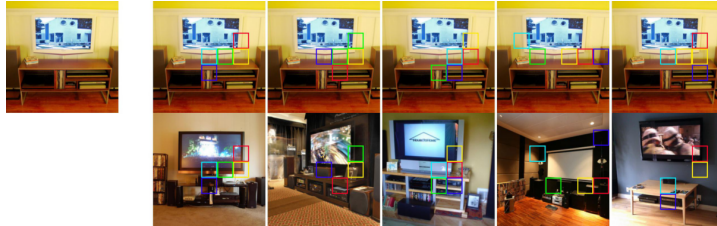


Query: ILSVRC2012_val_00025908.JPEG
 CHM Prediction: thatch
 Number of Users: 3
 Mean Accuracy: 0.0
 Real GT(s): hay

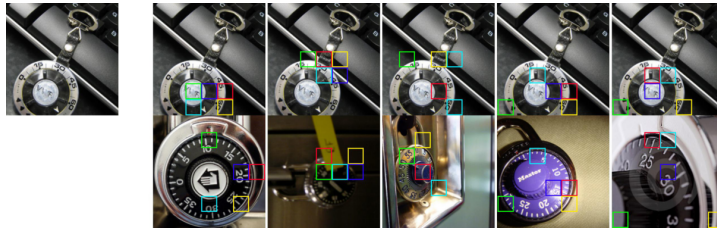


Figure A25: Accepting wrong CHM-Corr prediction due to confusing explanations

Query: ILSVRC2012_val_00021601.JPEG
 CHM Prediction: home theater
 Number of Users: 3
 Mean Accuracy: 0.0
 Real GT(s): entertainment center, monitor, desk, television



Query: ILSVRC2012_val_00018863.JPEG
 CHM Prediction: combination lock
 Number of Users: 3
 Mean Accuracy: 0.0
 Real GT(s): space bar, computer keyboard



Query: ILSVRC2012_val_00005467.JPEG
 CHM Prediction: stage
 Number of Users: 3
 Mean Accuracy: 0.0
 Real GT(s): electric guitar, microphone, acoustic guitar

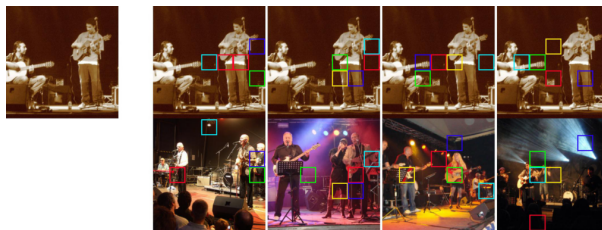


Figure A26: Accepting wrong CHM-Corr prediction due to poor ImageNet ReaL labeling

E.9 When explanations fool users

This section provides clear evidence that explanations have the potentials to fool human users. Both ResNet-50 and EMD-Corr misclassified an image of tow truck into cab. When asking a user to accept or reject this particular misclassification, they act differently based on the provided explanation. A total of 6 users who saw the query without any visual explanation were able to correctly reject AI's decision, while 3 out of 6 (50%) users who received either EMD-NN or EMD-Corr explanation incorrectly accepted the decision.

ResNet-50 Users: 3
EMD-NN Users: 2

ResNet-50 Human Accuracy: 100.0%
EMD-NN Human Accuracy: 50.0%

ResNet-50 output: cab
EMD-NN output: cab

Real GT(s): tow truck



ResNet-50 Users: 3
EMD-Corr Users: 4

ResNet-50 Human Accuracy: 100.0%
EMD-Corr Human Accuracy: 50.0%

ResNet-50 output: cab
EMD-Corr output: cab

Real GT(s): tow truck



Figure A27: Samples for human users failing to reject wrong AI decisions – A tow truck misclassified as a cab by EMD-Corr classifier.

F Classification accuracy of Human-AI teams

This section contains details on the Human and AI team’s complementary performance on different confidence thresholds T . For each threshold T , we divide the validation set into two groups; (1) images where the AI’s confidence is greater or equal to $\geq T$ and (2) images where the AI’s confidence is less than $< T$. In the first group, we only consider AI’s decision. For the second group, we ask a human user to judge AI’s predicted label, i.e., a human user should accept or reject AI’s classification.

Table A9: ResNet-50 - Aggregating Human and AI (%)

Threshold (T)	AI-alone confidence $\geq T$	Ratio of Images Handled by AI	Human accuracy confidence $< T$	Aggregate Human-AI accuracy	AI-alone confidence $\geq T$	Ratio of Images Handled by AI	Human accuracy confidence $< T$	Aggregate Human-AI accuracy
ImageNet					CUB			
0.00	83.14	1.0000	n/a	n/a	85.83	1.0000	n/a	n/a
0.05	83.18	0.9996	100.00	83.18	85.83	1.0000	n/a	n/a
0.10	83.42	0.9959	100.00	83.49	85.83	1.0000	n/a	n/a
0.15	83.96	0.9874	89.09	84.03	85.87	0.9991	100.00	85.88
0.20	84.65	0.9758	85.98	84.68	86.01	0.9967	76.47	85.98
0.25	85.44	0.9614	89.82	85.61	86.17	0.9933	79.49	86.12
0.30	86.35	0.9439	92.41	86.69	86.47	0.9888	83.93	86.44
0.35	87.32	0.9247	89.14	87.46	86.89	0.9819	76.40	86.70
0.40	88.29	0.9041	86.73	88.14	87.47	0.9722	72.17	87.04
0.45	89.38	0.8797	84.62	88.80	88.15	0.9570	69.36	87.34
0.50	90.47	0.8520	83.79	89.48	88.97	0.9392	65.38	87.54
0.55	91.56	0.8206	81.52	89.76	90.05	0.9173	59.27	87.50
0.60	92.59	0.7896	80.80	90.11	90.91	0.8947	60.78	87.74
0.65	93.55	0.7595	80.50	90.41	92.01	0.8723	57.23	87.56
0.70	94.50	0.7285	77.83	89.98	92.81	0.8469	54.56	86.95
0.75	95.38	0.6954	76.06	89.50	93.62	0.8198	54.60	86.59
0.80	96.21	0.6604	76.10	89.38	94.60	0.7891	52.55	85.73
0.85	96.99	0.6189	75.65	88.86	95.52	0.7551	51.72	84.79
0.90	97.82	0.5635	75.63	88.14	96.42	0.7090	51.91	83.47
0.95	98.67	0.4742	76.08	86.79	97.68	0.6108	54.55	80.89
1.00	n/a	0.0000	81.52	n/a	n/a	0.0000	65.50	n/a

Table A10: kNN - Aggregating Human and AI (%)

Threshold (T)	AI-alone confidence $\geq T$	Ratio of Images Handled by AI	Human accuracy confidence $< T$	Aggregate Human-AI accuracy	AI-alone confidence $\geq T$	Ratio of Images Handled by AI	Human accuracy confidence $< T$	Aggregate Human-AI accuracy
ImageNet					CUB			
0.00	82.14	1.0000	n/a	n/a	85.47	1.0000	n/a	n/a
0.05	82.16	0.9999	n/a	n/a	85.47	1.0000	n/a	n/a
0.10	82.52	0.9948	100.00	82.61	85.48	0.9998	n/a	n/a
0.15	83.34	0.9826	97.14	83.58	85.59	0.9986	100.00	85.61
0.20	84.36	0.9652	97.14	84.81	85.76	0.9962	100.00	85.81
0.25	85.67	0.9422	90.23	85.93	86.30	0.9886	68.18	86.09
0.30	86.85	0.9189	80.06	86.30	87.18	0.9720	50.70	86.16
0.35	88.10	0.8925	77.86	87.00	88.68	0.9455	47.83	86.45
0.40	89.44	0.8634	77.86	87.85	90.13	0.9115	47.83	86.39
0.45	90.67	0.8325	73.40	87.78	92.02	0.8673	50.85	86.56
0.50	91.91	0.7974	70.78	87.63	93.97	0.8101	50.70	85.76
0.55	93.06	0.7600	67.99	87.05	95.40	0.7618	47.31	83.95
0.60	94.24	0.7251	67.87	86.99	96.67	0.7152	47.39	82.63
0.65	95.25	0.6907	67.87	86.78	97.35	0.6700	47.39	80.86
0.70	96.15	0.6544	67.43	86.23	97.81	0.6215	49.68	79.59
0.75	96.91	0.6182	67.43	85.66	98.12	0.5687	49.68	77.23
0.80	97.57	0.5782	66.50	84.47	98.68	0.5109	51.14	75.43
0.85	98.10	0.5334	66.93	83.55	99.01	0.4550	52.95	73.91
0.90	98.72	0.4715	66.93	81.92	99.06	0.3871	52.95	70.80
0.95	99.19	0.3677	70.42	81.00	99.28	0.2858	58.60	70.23
1.00	n/a	0.0000	70.42	n/a	n/a	0.0000	58.60	n/a

Table A11: EMD-NN Aggregating Human and AI (%)

Threshold (T)	AI-alone confidence $\geq T$	Ratio of Images Handled by AI	Human accuracy confidence $< T$	Aggregate Human-AI accuracy	AI-alone confidence $\geq T$	Ratio of Images Handled by AI	Human accuracy confidence $< T$	Aggregate Human-AI accuracy
	ImageNet				CUB			
0.00	82.39	1.0000	n/a	n/a	84.98	1.0000	n/a	n/a
0.05	82.40	0.9999	n/a	n/a	84.98	1.0000	n/a	n/a
0.10	82.78	0.9945	100.00	82.88	85.01	0.9997	n/a	n/a
0.15	83.63	0.9819	96.10	83.86	85.15	0.9981	60.00	85.10
0.20	84.72	0.9636	96.10	85.13	85.34	0.9950	60.00	85.22
0.25	85.87	0.9424	95.24	86.41	85.98	0.9838	68.75	85.70
0.30	87.12	0.9186	88.36	87.22	87.03	0.9650	55.70	85.94
0.35	88.37	0.8914	83.11	87.80	88.39	0.9368	49.21	85.92
0.40	89.59	0.8625	83.11	88.70	90.19	0.8940	49.21	85.85
0.45	90.80	0.8319	81.49	89.24	92.40	0.8398	47.67	85.23
0.50	92.13	0.7956	77.45	89.13	94.47	0.7829	48.92	84.58
0.55	93.40	0.7576	73.59	88.60	95.74	0.7337	48.74	83.22
0.60	94.53	0.7211	70.41	87.80	96.45	0.6847	49.35	81.60
0.65	95.43	0.6858	70.41	87.56	97.35	0.6324	49.35	79.71
0.70	96.16	0.6502	68.68	86.55	97.89	0.5796	50.90	78.13
0.75	96.94	0.6130	68.68	86.01	98.17	0.5190	50.90	75.43
0.80	97.62	0.5709	68.46	85.11	98.77	0.4619	52.96	74.11
0.85	98.18	0.5232	69.70	84.60	99.30	0.3968	55.29	72.76
0.90	98.73	0.4579	69.70	82.99	99.34	0.3115	55.29	69.01
0.95	99.18	0.3524	73.15	82.33	99.38	0.1957	60.80	68.35
1.00	n/a	0.00	73.15	n/a	n/a	0.00	60.80	n/a

Table A12: EMD-Corr Aggregating Human and AI (%)

Threshold (T)	AI-alone confidence $\geq T$	Ratio of Images Handled by AI	Human accuracy confidence $< T$	Aggregate Human-AI accuracy	AI-alone confidence $\geq T$	Ratio of Images Handled by AI	Human accuracy confidence $< T$	Aggregate Human-AI accuracy
	ImageNet				CUB			
0.00	82.39	1.0000	n/a	n/a	84.98	1.0000	n/a	n/a
0.05	82.40	0.9999	n/a	n/a	84.98	1.0000	n/a	n/a
0.10	82.78	0.9945	100.00	82.88	85.01	0.9997	n/a	n/a
0.15	83.63	0.9819	95.29	83.84	85.15	0.9981	100.00	85.17
0.20	84.72	0.9636	95.29	85.10	85.34	0.9950	100.00	85.42
0.25	85.87	0.9424	95.57	86.43	85.98	0.9838	86.67	85.99
0.30	87.12	0.9186	89.27	87.29	87.03	0.9650	69.70	86.43
0.35	88.37	0.8914	85.19	88.02	88.39	0.9368	60.36	86.62
0.40	89.59	0.8625	85.19	88.98	90.19	0.8940	60.36	87.03
0.45	90.80	0.8319	82.59	89.42	92.40	0.8398	58.70	87.00
0.50	92.13	0.7956	79.17	89.48	94.47	0.7829	57.24	86.38
0.55	93.40	0.7576	74.67	88.86	95.74	0.7337	57.26	85.49
0.60	94.53	0.7211	72.40	88.36	96.45	0.6847	58.34	84.43
0.65	95.43	0.6858	72.40	88.19	97.35	0.6324	58.34	83.01
0.70	96.16	0.6502	70.44	87.16	97.89	0.5796	58.20	81.20
0.75	96.94	0.6130	70.44	86.69	98.17	0.5190	58.20	78.94
0.80	97.62	0.5709	70.71	86.08	98.77	0.4619	59.04	77.39
0.85	98.18	0.5232	71.74	85.57	99.30	0.3968	60.70	76.01
0.90	98.73	0.4579	71.74	84.10	99.34	0.3115	60.70	72.73
0.95	99.18	0.3524	74.63	83.28	99.38	0.1957	64.53	71.35
1.00	n/a	0.0000	74.63	n/a	n/a	0.0000	64.53	n/a

Table A13: CHM-NN Aggregating Human and AI (%)

Threshold (T)	AI-alone confidence $\geq T$	Ratio of Images Handled by AI	Human accuracy confidence $< T$	Aggregate Human-AI accuracy	AI-alone confidence $\geq T$	Ratio of Images Handled by AI	Human accuracy confidence $< T$	Aggregate Human-AI accuracy
ImageNet					CUB			
0.00	82.05	1.0000	n/a	n/a	83.28	1.0000	n/a	n/a
0.05	82.06	0.9999	n/a	n/a	83.28	1.0000	n/a	n/a
0.10	82.34	0.9960	n/a	n/a	83.29	0.9998	n/a	n/a
0.15	83.03	0.9853	94.74	83.20	83.36	0.9986	80.00	83.35
0.20	83.96	0.9695	94.74	84.28	83.56	0.9952	80.00	83.54
0.25	85.00	0.9507	88.97	85.20	84.30	0.9836	61.54	83.92
0.30	86.17	0.9286	81.37	85.82	85.64	0.9579	55.14	84.35
0.35	87.40	0.9035	80.58	86.75	87.25	0.9218	54.92	84.72
0.40	88.65	0.8760	80.58	87.65	89.63	0.8704	54.92	85.13
0.45	89.90	0.8455	79.22	88.25	91.81	0.8112	53.19	84.52
0.50	91.27	0.8085	77.88	88.71	94.17	0.7428	51.94	83.31
0.55	92.61	0.7706	73.72	88.27	96.15	0.6764	50.63	81.42
0.60	93.72	0.7348	69.48	87.29	97.22	0.6087	52.05	79.55
0.65	94.77	0.6996	69.48	87.18	97.84	0.5433	52.05	76.93
0.70	95.65	0.6657	68.99	86.74	98.43	0.4843	54.79	75.92
0.75	96.34	0.6300	68.99	86.22	98.71	0.4137	54.79	72.96
0.80	97.13	0.5904	69.23	85.70	98.83	0.3379	57.00	71.13
0.85	97.77	0.5432	68.79	84.53	99.26	0.2551	60.18	70.14
0.90	98.47	0.4812	68.79	83.07	99.34	0.1840	60.18	67.38
0.95	98.97	0.3796	71.49	81.92	99.64	0.0948	64.32	67.66
1.00	n/a	0.0000	71.49	n/a	n/a	0.0000	64.32	n/a

Table A14: CHM-Corr Aggregating Human and AI (%)

Threshold (T)	AI-alone confidence $\geq T$	Ratio of Images Handled by AI	Human accuracy confidence $< T$	Aggregate Human-AI accuracy	AI-alone confidence $\geq T$	Ratio of Images Handled by AI	Human accuracy confidence $< T$	Aggregate Human-AI accuracy
ImageNet					CUB			
0.00	82.05	1.0000	n/a	n/a	83.28	1.0000	n/a	n/a
0.05	82.06	0.9999	n/a	n/a	83.28	1.0000	n/a	n/a
0.10	82.34	0.9960	n/a	n/a	83.29	0.9998	n/a	n/a
0.15	83.03	0.9853	91.89	83.16	83.36	0.9986	100.00	83.38
0.20	83.96	0.9695	91.89	84.20	83.56	0.9952	100.00	83.64
0.25	85.00	0.9507	86.99	85.10	84.30	0.9836	53.85	83.80
0.30	86.17	0.9286	81.90	85.86	85.64	0.9579	72.22	85.07
0.35	87.40	0.9035	78.35	86.53	87.25	0.9218	71.06	85.98
0.40	88.65	0.8760	78.35	87.37	89.63	0.8704	71.06	87.22
0.45	89.90	0.8455	77.39	87.97	91.81	0.8112	63.58	86.48
0.50	91.27	0.8085	76.85	88.51	94.17	0.7428	62.92	86.13
0.55	92.61	0.7706	73.35	88.19	96.15	0.6764	61.15	84.82
0.60	93.72	0.7348	70.30	87.51	97.22	0.6087	60.52	82.86
0.65	94.77	0.6996	70.30	87.42	97.84	0.5433	60.52	80.79
0.70	95.65	0.6657	70.21	87.15	98.43	0.4843	62.36	79.83
0.75	96.34	0.6300	70.21	86.67	98.71	0.4137	62.36	77.40
0.80	97.13	0.5904	70.56	86.24	98.83	0.3379	63.37	75.35
0.85	97.77	0.5432	69.32	84.78	99.26	0.2551	65.20	73.89
0.90	98.47	0.4812	69.32	83.35	99.34	0.1840	65.20	71.48
0.95	98.97	0.3796	71.30	81.80	99.64	0.0948	68.29	71.26
1.00	n/a	0.0000	71.30	n/a	n/a	0.0000	68.29	n/a

G Analysis for CUB

G.1 Correspondences help users to reject wrong AI prediction

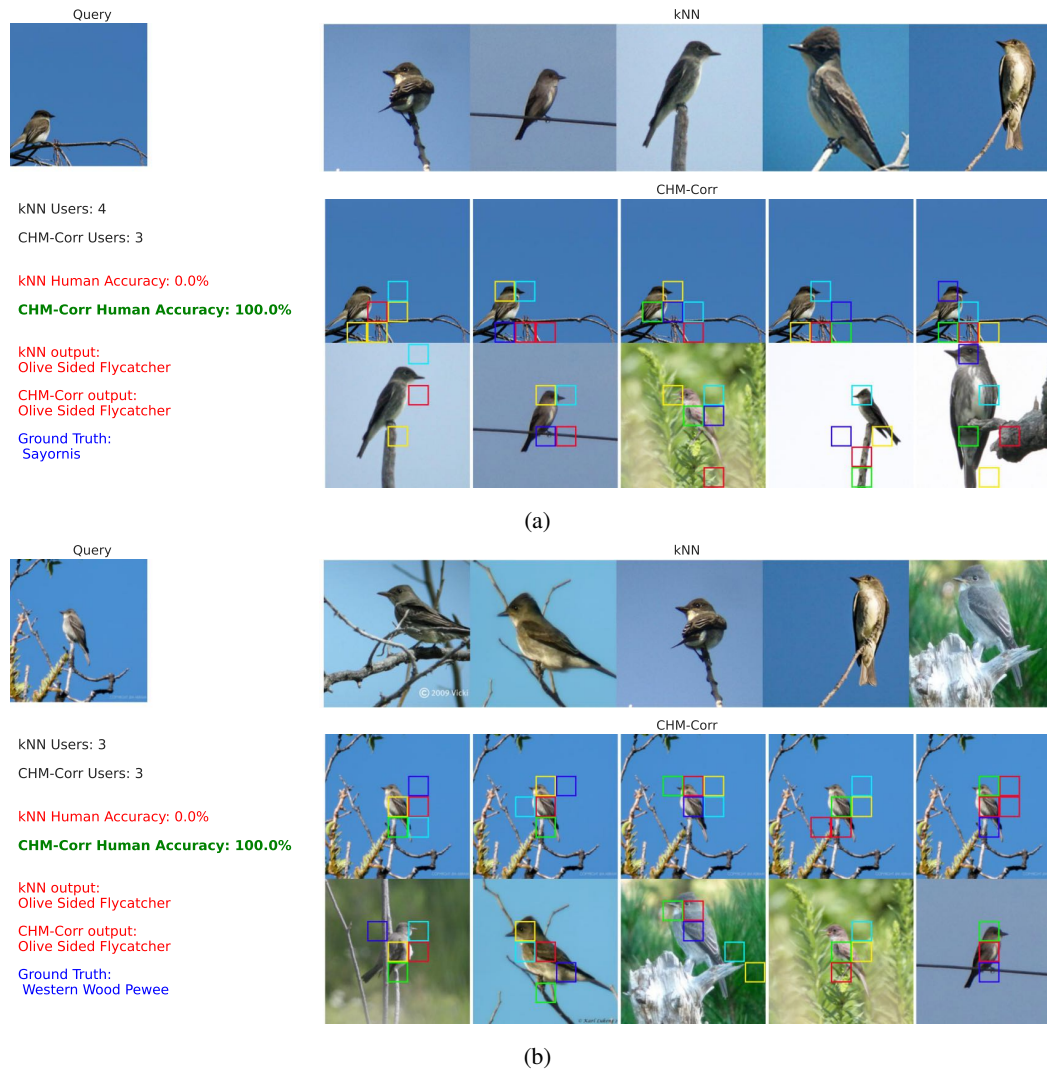


Figure A28: When correspondences help users to reject wrong AI prediction – (a) Both kNN and CHM-Corr classifiers misclassified an image of Sayornis into Olive Sided Flycatcher. Using kNN explanations, 4/4 of users failed to reject this wrong prediction, while using CHM-Corr explanations, 3/3 of users successfully rejected AI decisions. (b) Both kNN and CHM-Corr classifiers misclassified an image of Western Wood Pewee into Olive Sided Flycatcher. Using kNN explanations, 3/3 of users failed to reject this wrong prediction, while using CHM-Corr explanations, 3/3 of users successfully rejected AI decisions.

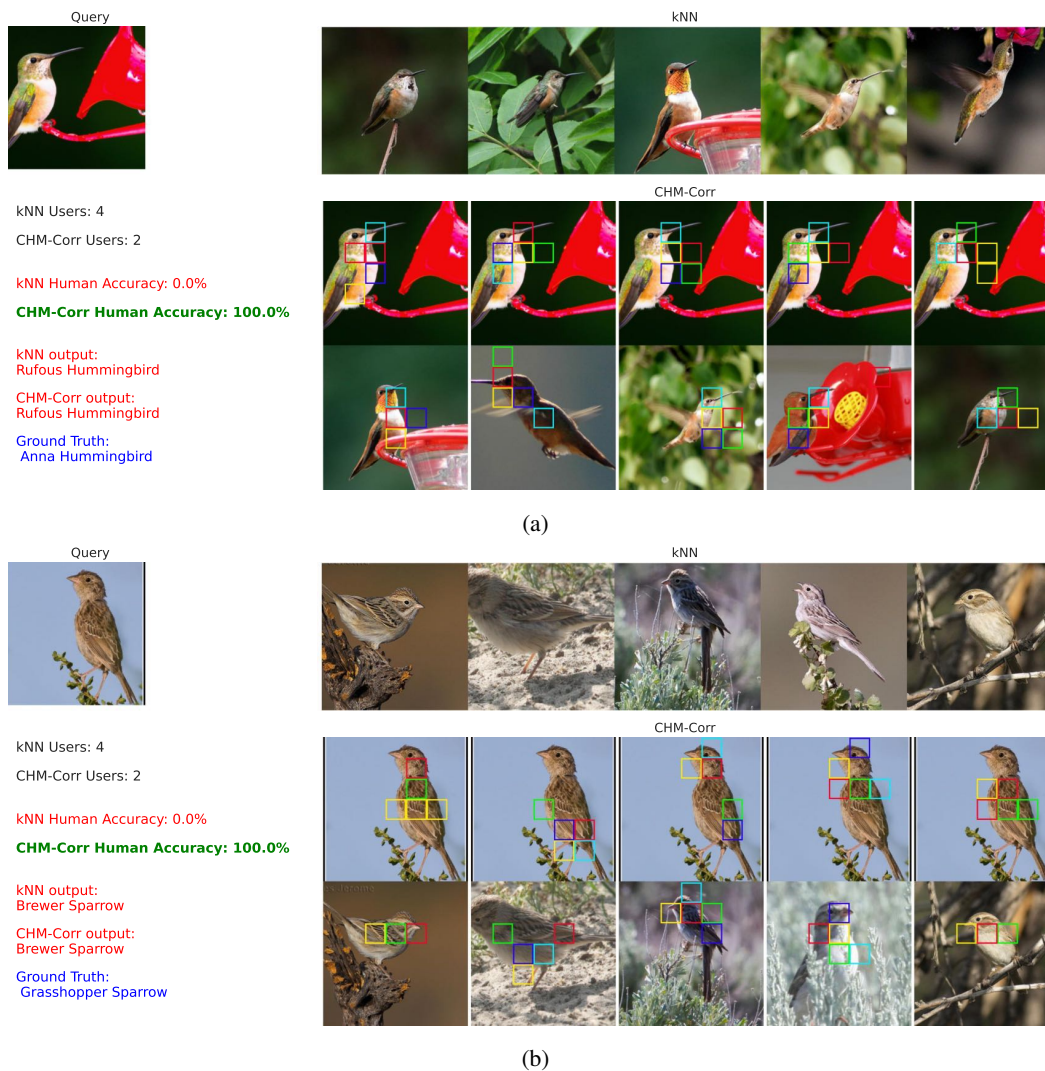


Figure A29: When correspondences help users to reject wrong AI prediction – **(a)** Both kNN and CHM-Corr classifiers misclassified an image of Anna Hummingbird as a Rufous Hummingbird. Using kNN explanations, 4/4 of users failed to reject this wrong prediction, while using CHM-Corr explanations, 2/2 of users successfully rejected AI decisions. **(b)** Both kNN and CHM-Corr classifiers misclassified an image of Grasshopper Sparrow as a Brewer Sparrow. Using kNN explanations, 4/4 of users failed to reject this wrong prediction, while using CHM-Corr explanations, 2/2 of users successfully rejected AI decisions.

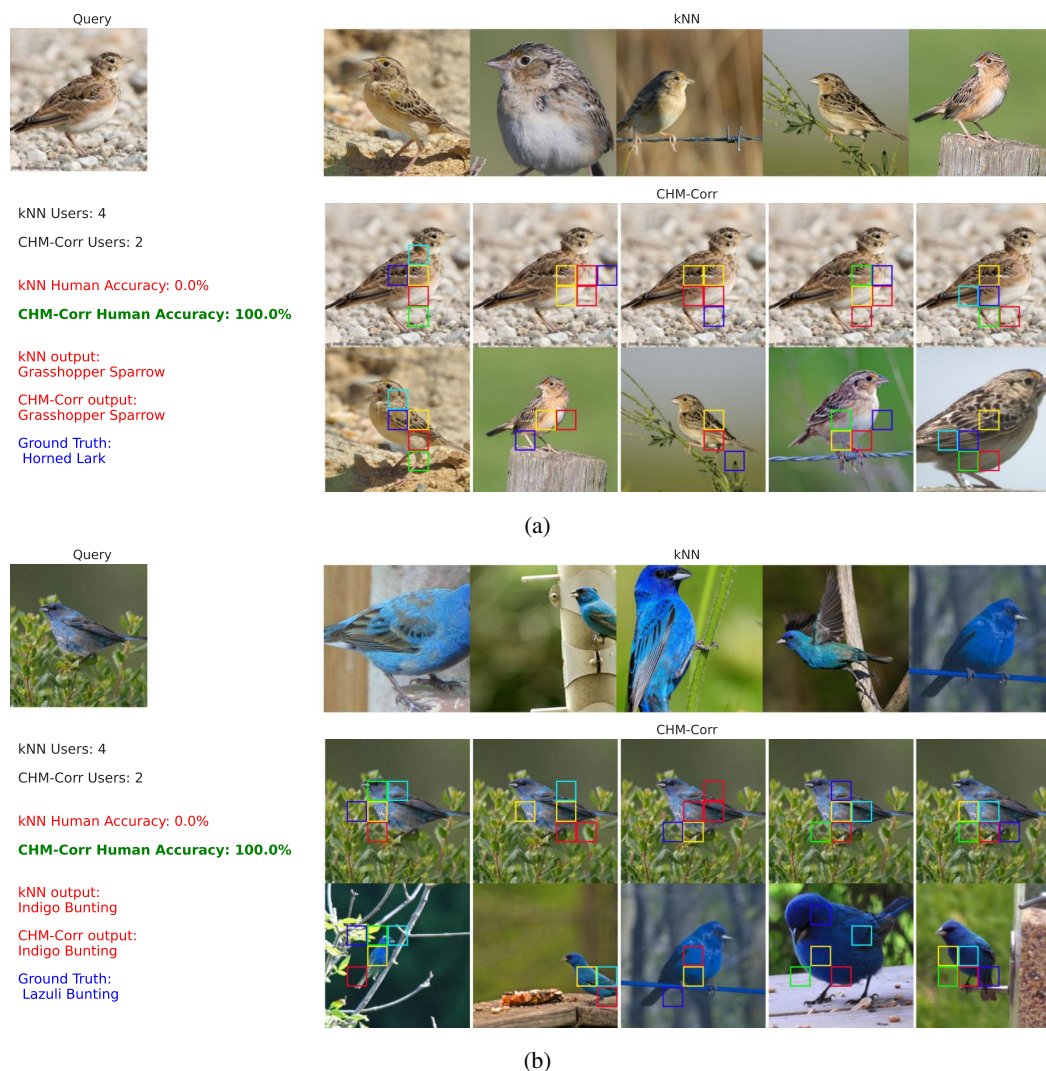
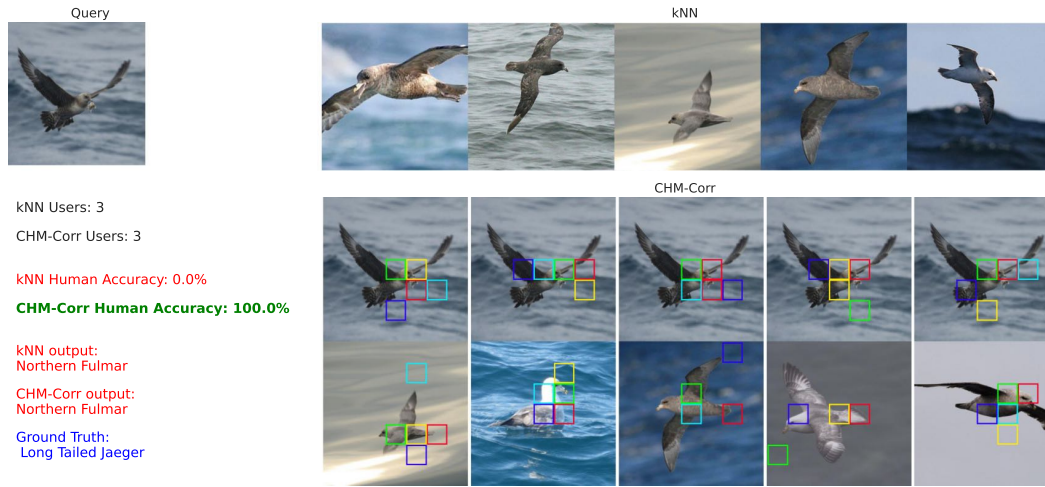
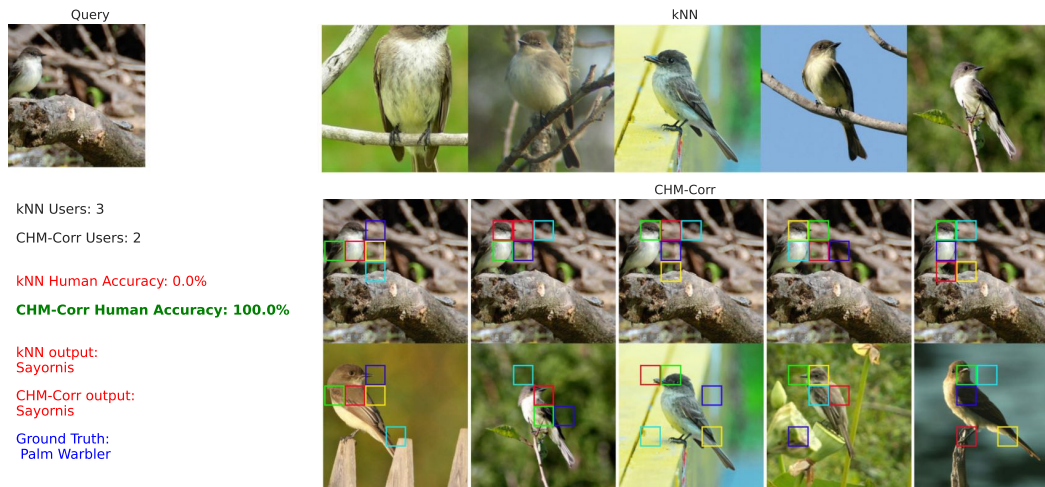


Figure A30: When correspondences help users to reject wrong AI prediction – **(a)** Both kNN and CHM-Corr classifiers misclassified an image of Horned Lark as a Grasshopper Sparrow. Using kNN explanations, 4/4 of users failed to reject this wrong prediction, while using CHM-Corr explanations, 2/2 of users successfully rejected AI decisions. **(b)** Both kNN and CHM-Corr classifiers misclassified an image of Lazuli Bunting as an Indigo Bunting. Using kNN explanations, 4/4 of users failed to reject this wrong prediction, while using CHM-Corr explanations, 2/2 of users successfully rejected AI decisions.



(a)



(b)

Figure A31: When correspondences help users to reject wrong AI prediction – (a) Both kNN and CHM-Corr classifiers misclassified an image of Long Tailed Jaeger as a Northern Fulmar. Using kNN explanations, 3/3 of users failed to reject this wrong prediction, while using CHM-Corr explanations, 3/3 of users successfully rejected AI decisions. (b) Both kNN and CHM-Corr classifiers misclassified an image of Palm Warbler as a Sayornis. Using kNN explanations, 3/3 of users failed to reject this wrong prediction, while using CHM-Corr explanations, 2/2 of users successfully rejected AI decisions.

G.2 Diversity of images in kNN and, EMD-Corr, and CHM-Corr explanations

We hypothesize that when the AI prediction is wrong, the diversity among the five nearest neighbors of kNN differs from EMD-Corr and CHM-Corr, leading to users rejecting the decision. To this end, we calculated LPIPS and MS-SSIM metrics between all possible pairs of explanations on the relevant queries.

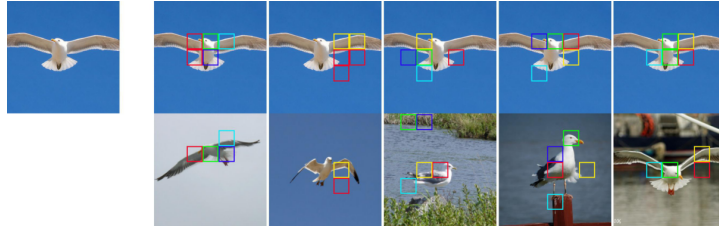


Figure A32: Analysis of the diversity between all 10 possible pairs of five nearest neighbors for queries with the average user's accuracy of 0% when kNN explanation is provided and the average user's accuracy of 100% when CHM-Corr explanation is provided (CUB). **The images in kNN explanations are consistently less diverse under both LPIPS (a) and MS-SSIM (b) than those in EMD-Corr and CHM-Corr explanations.** That is, this is evidence explaining why kNN users tend to be fooled into accepting kNN wrong the decisions the most.

G.3 When the user rejects the correct AI prediction

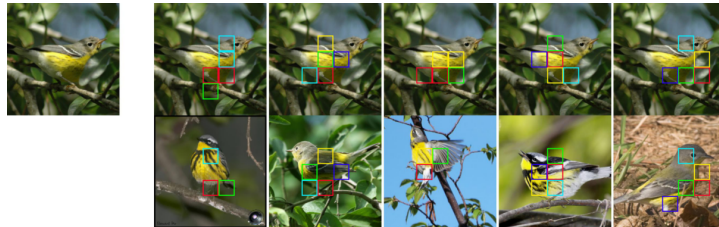
This section provides a brief qualitative explanation for the cases that users incorrectly rejected a correct AI prediction.

Query: California_Gull_0132_40836
CHM Prediction: California Gull
Users: 3
Accuracy: 0



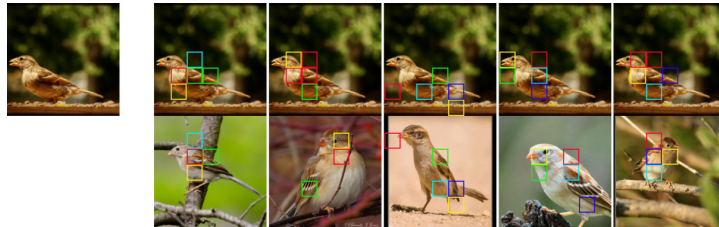
(a) The CHM-Corr classifier missed tips at wings, and the legs' black tips were occluded.

Query: Magnolia_Warbler_0021_165919
CHM Prediction: Magnolia Warbler
Users: 2
Accuracy: 0



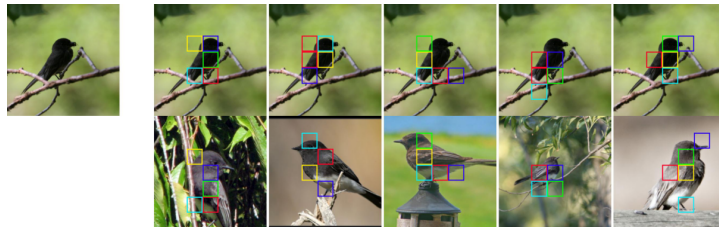
(b) The CHM-Corr classifier missed the stripes at the belly.

Query: Field_Sparrow_0092_113580
CHM Prediction: Field Sparrow
Users: 3
Accuracy: 0



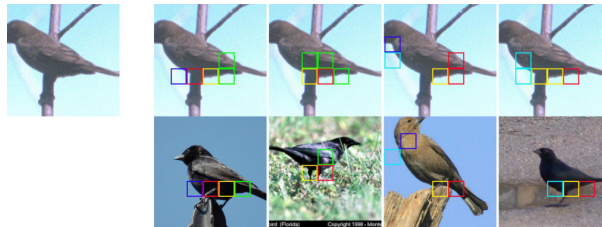
(c) Low-quality query – No distinctive features can be recognized from the input image.

Query: Sayornis_0030_98343
CHM Prediction: Sayornis
Users: 3
Accuracy: 0



(d) Low-quality query – No distinctive features can be recognized from the input image.

Query: Shiny_Cowbird_0043_796857
CHM Prediction: Shiny Cowbird
Users: 3
Accuracy: 0



(e) Low-quality query – No distinctive features can be recognized from the input image.

Figure A33: Analysis of queries that user's rejected correct CHM-Corr prediction.

H Comparing explanation methods

This section compares explanations provided by kNN, EMD-Corr, and CHM-Corr for various sets of queries.

H.1 ImageNet samples

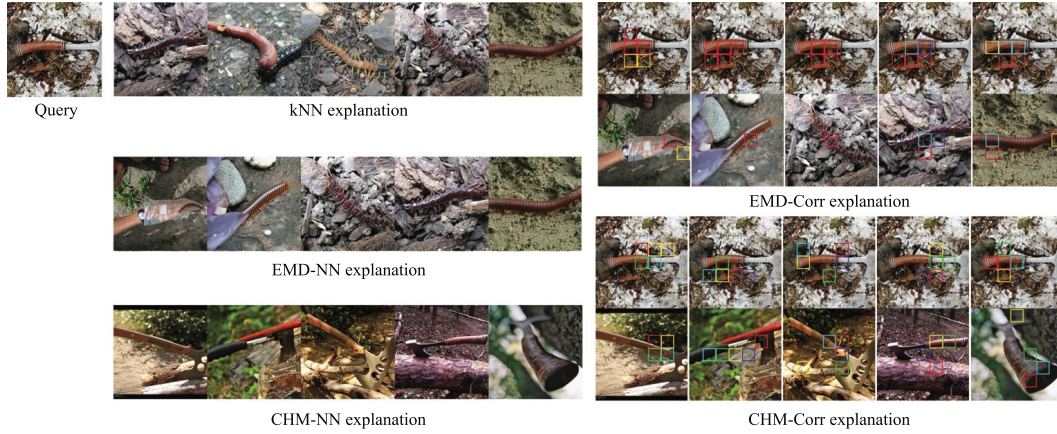


Figure A34: The kNN and EMD-Corr misclassify an image of hatchet as a centipede. The CHM-Corr correctly classifies this image.

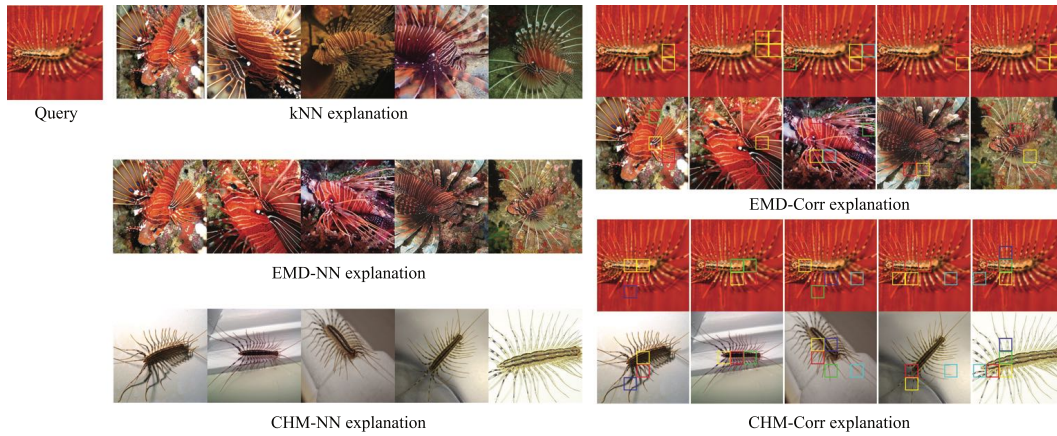


Figure A35: The kNN and EMD-Corr misclassify an image of centipede as a lionfish due to the dominant red color in the background. The CHM-Corr correctly classifies this image.

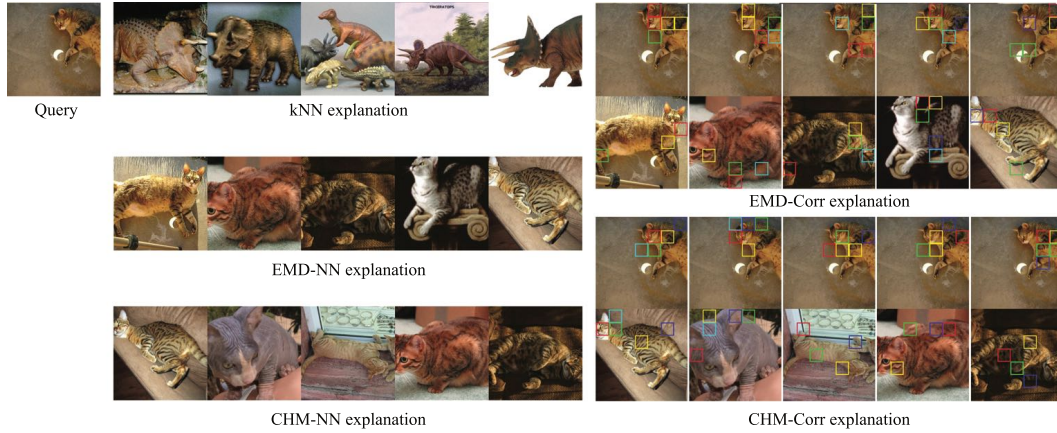


Figure A36: The kNN misclassifies an ImageNet image of tiger cat into triceratops. The EMD-Corr and CHM-Corr are both correctly classifying this image.

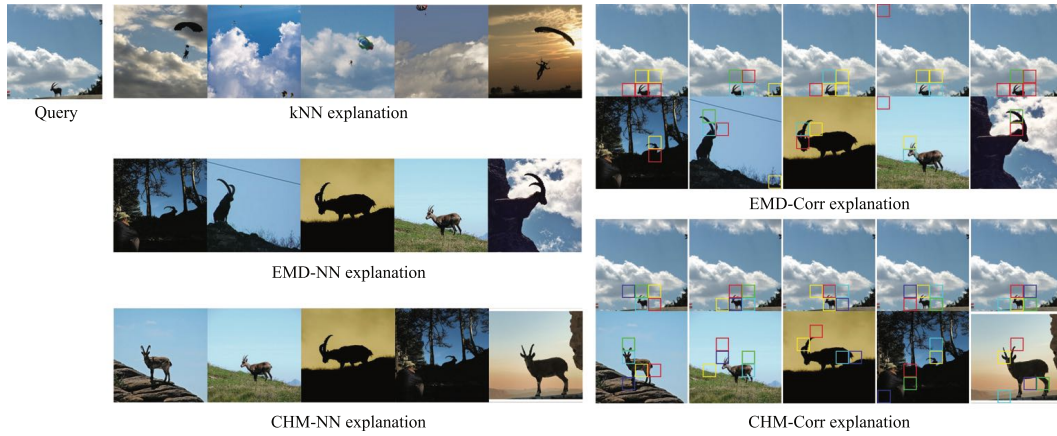


Figure A37: The kNN misclassifies an image of ibex as a parachute due to the dominant background. The EMD-Corr and CHM-Corr are both correctly classifying this image.

H.2 Adversarial samples

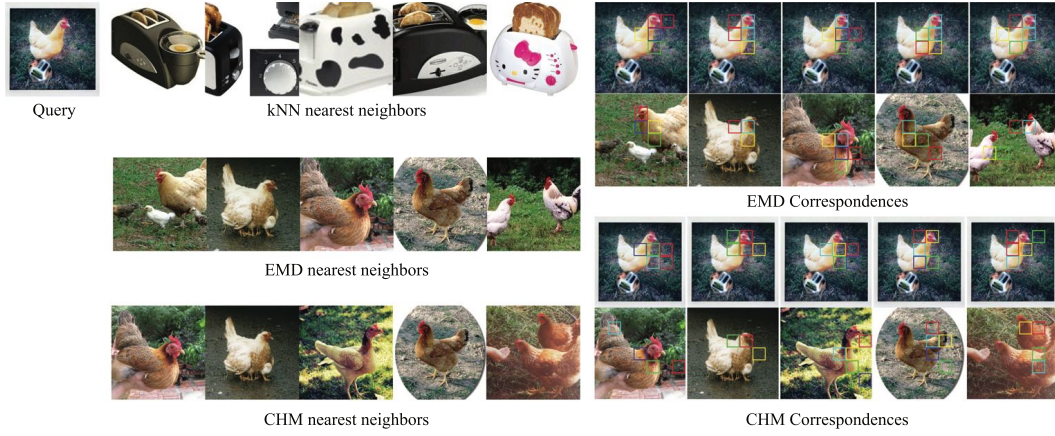


Figure A38: The kNN misclassifies an image of hen as a toaster due to an adversarial patch. The EMD-Corr and CHM-Corr are both correctly classifying this image.

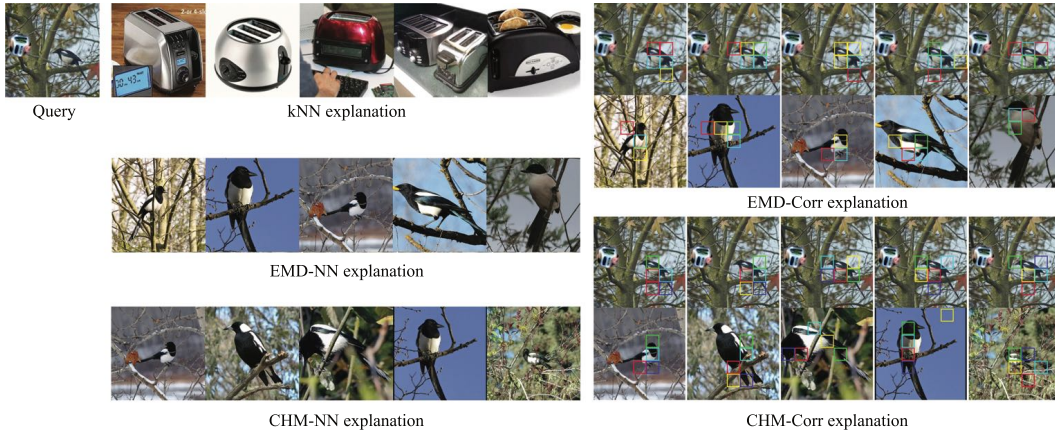
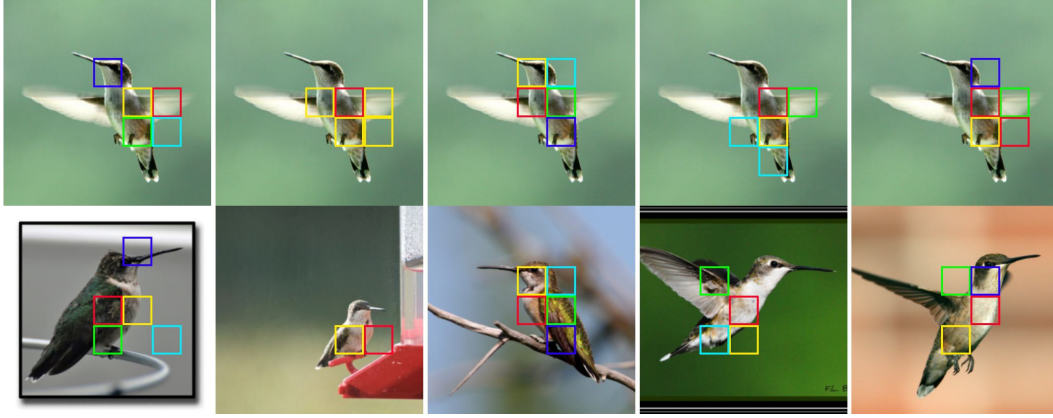


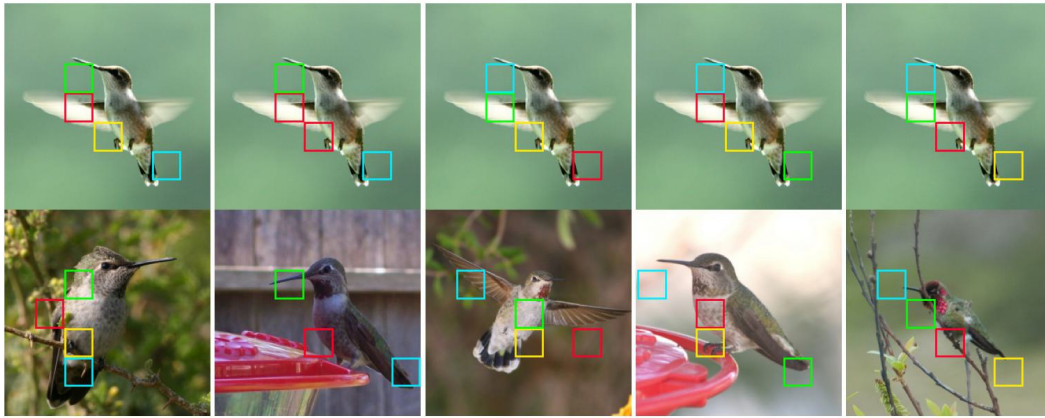
Figure A39: The kNN misclassifies an image of magpie as a toaster due to adversarial patch. The EMD-Corr and CHM-Corr are both correctly classifying this image.

I Controlling keypoints in CHM-Corr+ for the CUB dataset

Here, we compare CHM-Corr and CHM-Corr+ classifiers to understand the low performance of CHM-Corr+. Using a set of **five** keypoints may not help CHM-Corr+ focus on the right patches. Sometimes, the five provided keypoints are not among the discriminative features to correctly classify a bird.

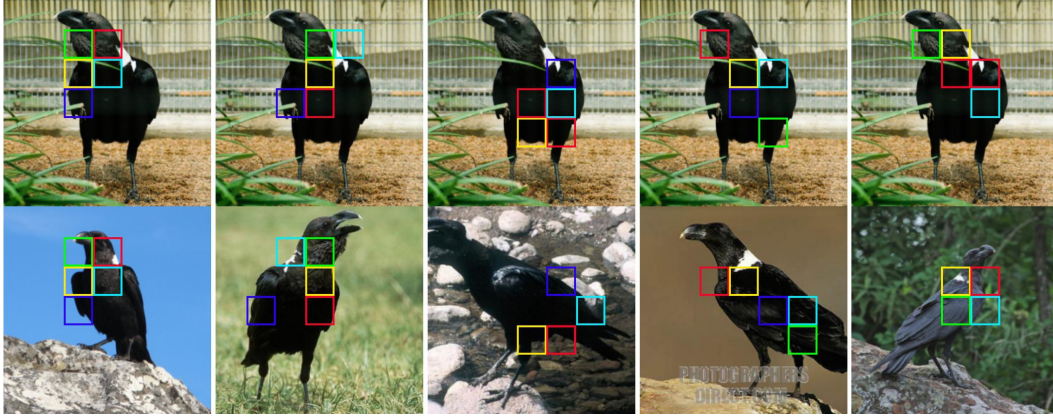


(a) The explanation of a **correct** classification by CHM-Corr.

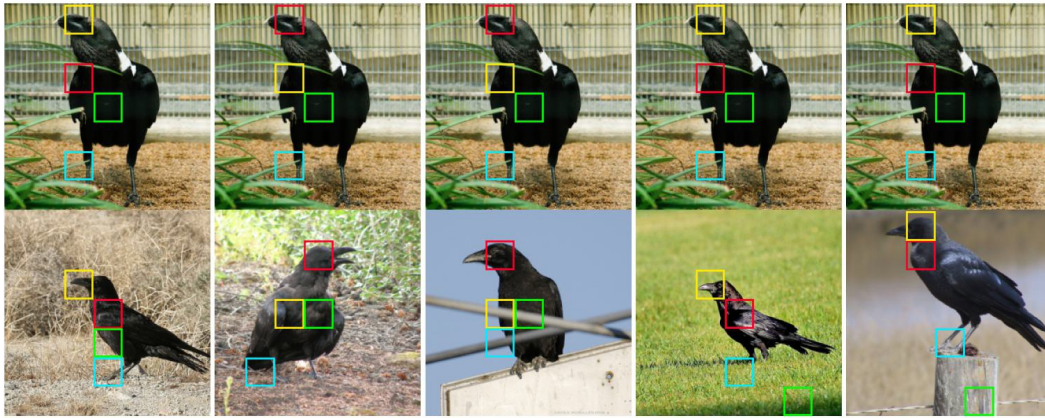


(b) The explanation of a **misclassification** by CHM-Corr+

Figure A40: A Ruby-throated Hummingbird misclassified into Anna Hummingbird by CHM-Corr+. An example of low-quality keypoints leading to selecting and comparing mostly background (uninformative) patches.

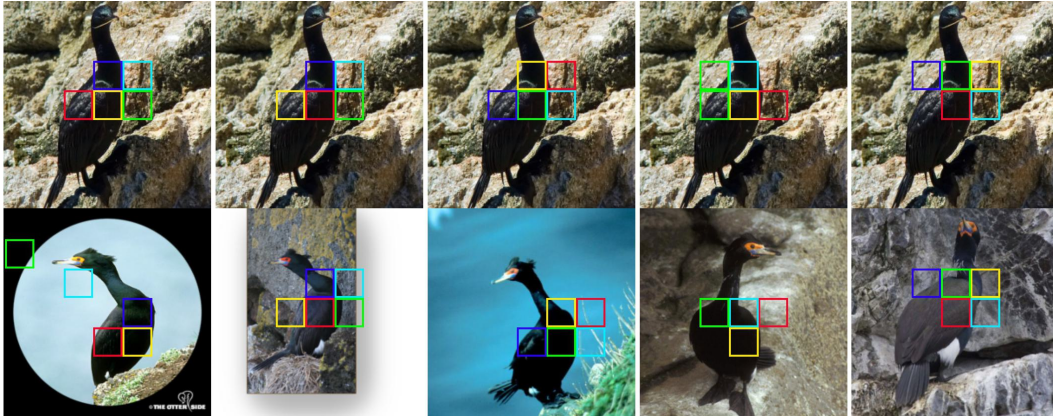


(a) The explanation of a **correct** classification by CHM-Corr.

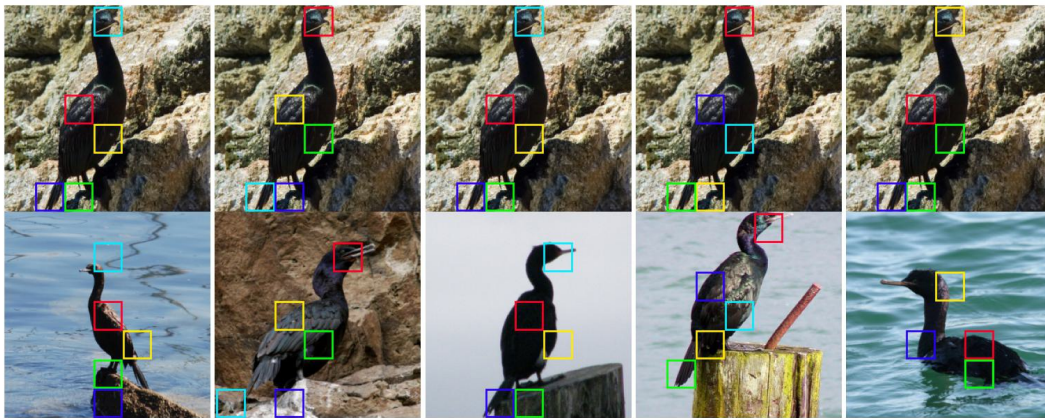


(b) The explanation of a **misclassification** by CHM-Corr+.

Figure A41: A White necked Raven misclassified as a Common Raven by CHM-Corr+. – The distinctive part of the bird is ‘the white feathers on the neck’, which is missed in the keypoints selection step in the CHM-Corr+. The CHM-Corr classifier correctly classifies this image.



(a) The explanation of a **misclassification** by CHM-Corr



(b) The explanation of a **correct** prediction by CHM-Corr+.

Figure A42: A Pelagic Cormorant misclassified as a Red Faced Cormorant by CHM-Corr. The face of the bird was not among the top-5 correspondences picked by CHM-Corr, which led to misclassification. The CHM-Corr+ classifier correctly classifies this image.

J Samples for ImageNet-Sketch dataset



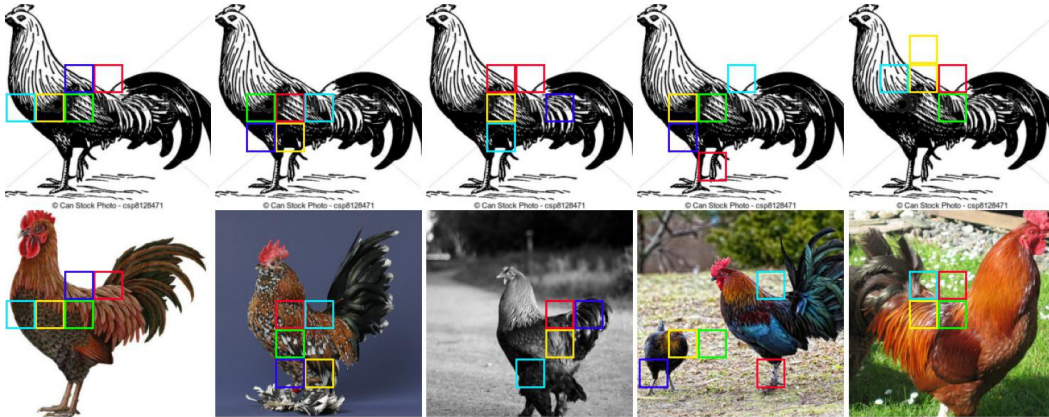
(a) Query – Cock



(b) Nearest neighbors using kNN

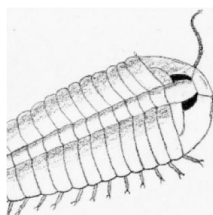


(c) Nearest neighbors after re-ranking using CHM-Corr



(d) CHM-Corr explanation

Figure A43: A **misclassification** by the kNN classifier. The black-and-white stripe patterns in cock confuse the kNN classifier, while the CHM-Corr classifier correctly labels the query.



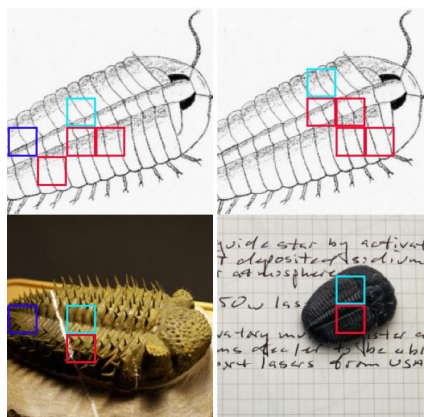
(a) Query – Trilobite



(b) Nearest neighbors using kNN



(c) Nearest neighbors after re-ranking using CHM-Corr



(d) CHM-Corr explanation

Figure A44: A **misclassification** by the kNN classifier. An image of trilobite misclassified as a chainlink fence by the kNN classifier, while the CHM-Corr classifier correctly classifies the query. The confidence of CHM-Corr is only 2/20, i.e., 10%. That is, there are only two trilobite images among the top-20 candidates.

K Removing duplicated images from ImageNet validation set

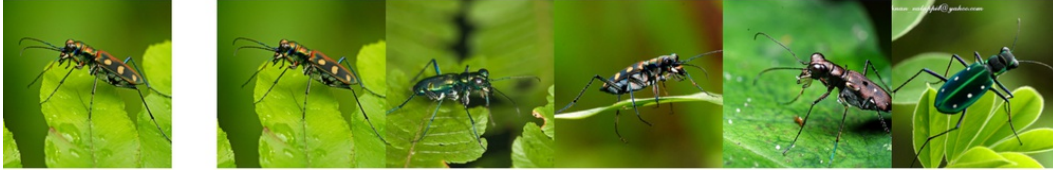
Some of the images from the ImageNet validation set are also present in the training set. For the human study, we excluded such images from our study. Figure A45, shows some of these samples along with their five nearest neighbor images from the training set.



(a) Query: ILSVRC2012_val_00009877 . JPEG



(b) Query: ILSVRC2012_val_00017380 . JPEG



(c) Query: ILSVRC2012_val_00020013 . JPEG



(d) Query: ILSVRC2012_val_00024875 . JPEG



(e) Query: ILSVRC2012_val_00046136 . JPEG



(f) Query: ILSVRC2012_val_00014815 . JPEG

Figure A45: In each panel, the leftmost image is in the validation set and the top-5 nearest images on the right are from the training set. We find images that exist both in the training set and validation set and remove them from our validation set (in order to not unfairly favor kNN in the study).